

**UC Davis**

**UC Davis Electronic Theses and Dissertations**

**Title**

Wine Stabilization of Potassium Bitartrate in a Fluidized Bed Crystallizer

**Permalink**

<https://escholarship.org/uc/item/2bf2s0g0>

**Author**

Geveke, Benjamin

**Publication Date**

2021

Peer reviewed|Thesis/dissertation

Wine Stabilization of Potassium Bitartrate in a Fluidized Bed Crystallizer

By

BENJAMIN GEVEKE  
THESIS

Submitted in partial satisfaction of the requirements for the degree of

MASTER OF SCIENCE

in

Chemical Engineering

in the

OFFICE OF GRADUATE STUDIES

of the

UNIVERSITY OF CALIFORNIA

DAVIS

Approved:

---

Ron Runnebaum, Chair

---

Ahmet Palazoglu

---

Robert Coleman

Committee in Charge

2021

## **Abstract**

Cold stabilization of potassium bitartrate is a common practice in wine production, however it is time and energy intensive due to the low temperatures required to facilitate crystallization. It has been demonstrated that a fluidized bed crystallizer could perform the same function as cold stabilization while minimizing drawbacks from batch operation. Two bench scale fluidized beds were constructed and tested with several size fractions of potassium bitartrate crystals in a model wine solution to isolate the parameters to determine bed height expansion. It was found that tube diameter and mass of loading showed little difference between scales, and that the crystal shape and size played a larger role. A pilot-scale fluidized bed crystallizer was designed and tested on an unstable wine to remove potassium bitartrate. The crystallizer selectively removed potassium bitartrate, confirmed by a decrease in conductivity, chemical analysis using HPLC, and particle analysis before and after fluidization. These results provide a positive step in designing a more efficient semi-continuous approach to remove potassium bitartrate analogous to cold stabilization.

## Table of Contents

<b>Abstract</b> .....	<b>ii</b>
<b>Notation</b> .....	<b>v</b>
<b>Acknowledgements</b> .....	<b>vi</b>
<b>Chapter 1. The Current State of Potassium Bitartrate Stabilization in Wine</b> .....	<b>1</b>
1.1. Overview .....	1
1.2. Potassium Bitartrate Instability .....	1
1.4. Fluidized Beds .....	4
1.5. Electrodialysis .....	6
1.6. Ion-Exchange .....	8
1.7. Continuous Bitartrate Stabilization Methods .....	9
1.8. Additives for Stabilization .....	10
1.8.1 Carboxymethyl Cellulose .....	10
1.8.2 Metatartaric Acid .....	10
1.8.3 Yeast Mannoproteins .....	11
1.8.4 Potassium Polyaspartate .....	11
1.9. Summary .....	12
<b>Chapter 2. An Investigation of the Hydrodynamic Behavior of Potassium Bitartrate Crystals in Model Fluidized Beds</b> .....	<b>13</b>
2.1. Overview .....	13
2.2. Introduction .....	13
2.3. Materials and Methods .....	17
2.3.1 Bench-scale Fluidized Beds.....	17
2.3.2 Potassium Bitartrate Crystals.....	18
2.3.3 Model Wine Solution.....	20
2.3.4 Measurements .....	20
2.4. Results and Discussion.....	21
2.4.1 Particle Analysis .....	21
2.4.2 Fluidization Analysis .....	24
2.5. Summary .....	29
<b>Chapter 3. The Removal of Potassium Bitartrate in a Pilot-scale Fluidized Bed Crystallizer</b> .....	<b>30</b>
3.1. Overview .....	30

3.2. Introduction .....	30
3.2.1 Crystallization.....	30
3.2.1 HPLC .....	31
3.3. Materials and Methods.....	31
3.3.1 The Development of a Pilot-scale Fluidized Bed Crystallizer .....	31
3.3.2 HPLC .....	34
3.3.3 Particle analysis .....	35
3.3.4 Potassium Bitartrate Stability .....	35
3.3.5. Experimental Procedure .....	35
3.4. Results and Discussion.....	36
<b>Conclusion .....</b>	<b>44</b>
<b>References .....</b>	<b>45</b>
<b>Supplemental Figures .....</b>	<b>48</b>

## Notation

Symbol	Meaning
$\varepsilon$	Bed voidage
$u_s$	Superficial fluid velocity
$t_r$	Residence time
$h$	Bed height
$u_{mf}$	Minimum fluidization velocity
$d_p$	Particle diameter
$\phi$	Particle sphericity
$D_p$	Modified particle diameter
$D$	Column diameter
$Q$	Flow rate
$P$	Perimeter of particle
$C$	Particle circularity
$\varepsilon_0$	Unexpanded bed voidage
$\mu$	Fluid dynamic viscosity
$\rho_s$	Particle density
$\rho_f$	Fluid density
$\nu$	Fluid kinematic viscosity
$F_{max}$	Maximum Feret diameter
$F_{min}$	Minimum Feret diameter
$u_t$	Particle terminal velocity
$Re_p$	Particle Reynolds number

## **Acknowledgements**

I would like to thank those who have helped me complete this project and have supported me over the years: My professor, Ron Runnebaum, for his patience, guidance, and understanding. The many members of Beringer Winery who devoted hours of their time and expertise in the fabrication and operation of the fluidized bed crystallizer, without which this research would not be possible. Professor Emeritus Roger Boulton, whose ideas continue to contribute to this field. My undergraduate lab member, Leo Jayachandran, for his assistance in experimentation and Python coding. My committee members, Ahmet Palazoglu and Robert Coleman, for their support and knowledge. Treasury Wine Estates, for help funding this research. And to my friends and family for keeping me going through the toughest days.

# **Chapter 1. The Current State of Potassium Bitartrate Stabilization in Wine\***

## **1.1. Overview**

The most common method to treat potassium bitartrate instability today is batch cold stabilization. Wine is transferred into cold jacketed tanks and the temperature is reduced until potassium bitartrate crystallizes out of solution, which may take up to two weeks. Cooling and maintaining large volumes of wine is heavily energy intensive. Cold stabilization includes cleaning the tartrate deposits on tank surfaces with hot water and caustic chemicals and a loss of some product as waste. As energy, water, and treatment costs continue to rise, it is practical to consider alternative practices.

Technologies from other applications can be adapted to remove potassium bitartrate from wine. The past two decades have also seen an increase in the variety of anti-crystallization additives approved for use in wine. This chapter aims to introduce the major alternative options wineries could use to replace cold stabilization.

## **1.2. Potassium Bitartrate Instability**

A clear, consistent, stabilized product is expected of most commercial wines. A 2015 survey reported that 40% of American wine consumers would not buy a wine again that displayed any form of precipitation.<sup>2</sup> Although potassium bitartrate crystals that appear in wine are not harmful, they can easily be mistaken for shards of broken glass. To avoid this misunderstanding, most wineries will ensure stabilization before the wine is bottled and shipped.

---

\* This chapter has been published in *Catalyst: Discovery into Practice*, by Geveke, B. and Runnebaum, R. C. The Future of Potassium Bitartrate Stabilization: Minimizing Energy Usage, Wine Loss and Treatment Time.<sup>1</sup> The original manuscript has been rearranged to fit this thesis.



Potassium bitartrate is a natural product of grapes and can crystallize in wine. Solubility is high in grape juice and the salt exists as two ions, potassium ( $K^+$ ) and bitartrate ( $C_4H_5O_6^-$ ). Two factors lower the solubility in wine and lead to crystal formation: lower polarity, and low temperatures.<sup>3</sup> During fermentation, ethanol is produced from sugar and changes the chemical polarity of the liquid. Potassium bitartrate is less soluble in ethanol than water and precipitates out of solution as the ethanol concentration rises.<sup>4</sup> Solubility is highly dependent on the temperature of the liquid. For example, a decrease in temperature from 15°C (59°F) to 0°C (32°F) in a 12% ethanol/water solution results in a 50% decrease of soluble salt, leading the rest to crystallize.<sup>4</sup> Lowering the temperature of an untreated wine, such as during transportation in winter or in a consumer's refrigerator, risks precipitation of crystals in the bottle. In order to stabilize, there are two broad approaches: subtractive, in which potassium bitartrate is removed, and additive, in which compounds are added to hinder potassium bitartrate crystallization.

### **1.3. Cold Stabilization**

Batch cold stabilization is the most widespread potassium bitartrate stabilization technique used, shown schematically in Figure 1. A jacketed tank lowers the temperature of an unstable wine to 0°C or below. Potassium bitartrate crystallizes and precipitates in the tank until solubility equilibrium is met. This process may take several days to several weeks because of the slow crystallization and settling conditions in large tanks.<sup>5</sup> The crystallization process can be expedited by adding cream of tartar (powdered potassium bitartrate) which provides a favorable surface for crystallization.

Refrigeration, which cold stabilization is a part of, can account for 50 - 70% of the total electricity used by a winery.<sup>6</sup> Wineries operating on a central refrigeration plant need to lower the

entire system to cold stabilization temperatures, even if only one tank in the winery needs treatment. Tanks with low insulation values compound the waste of energy.

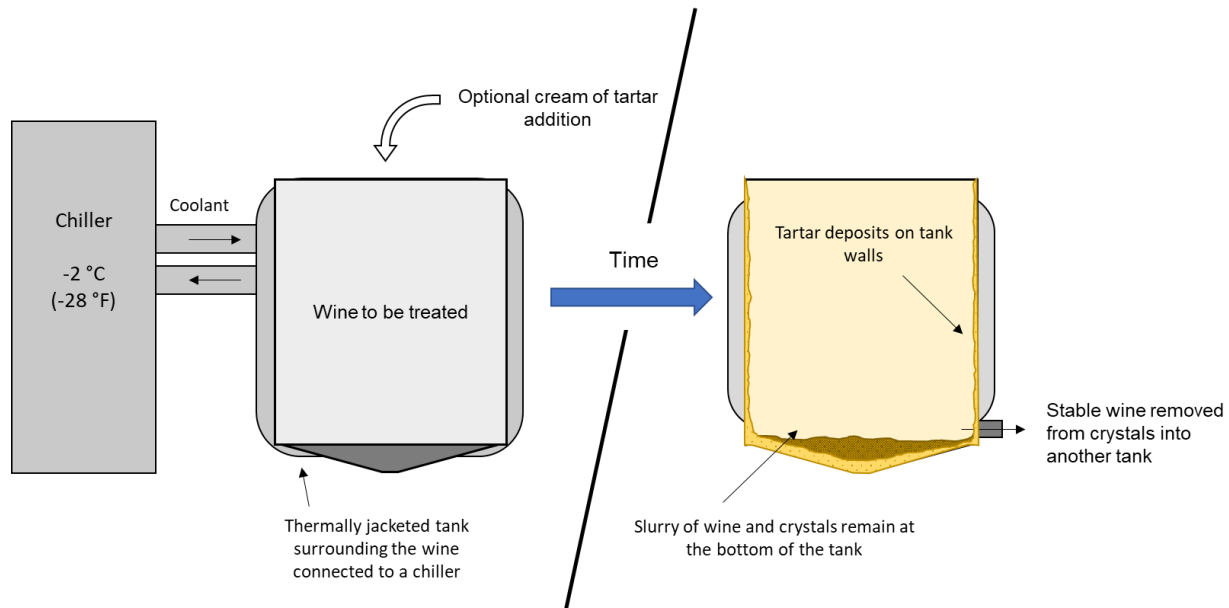


**Figure 1.** Schematic of cold stabilization. Wine is chilled in a jacketed tank and then removed from the crystals once stabilization has been reached.

Once a wine is determined to be stable it is racked into a clean receiving tank. The stabilized wine has a lower concentration of potassium and bitartrate ions that will not crystalize if brought back to the same cold temperature. The crystals remain in a slurry in the bottom of the tank, accounting for wine loss that can depend upon tank dimensions and amount of precipitate. In a study by the Australian Wine Research Institute, wine loss from batch cold stabilization was 1.45% the volume of wine treated in a tank.<sup>7</sup> It has been estimated that wine loss could be lowered to 0.4% if a centrifuge was used to recover wine from the crystals; although the recovered wine would be sold as a downgraded product.<sup>8</sup>

Although a simple treatment, batch cold stabilization has drawbacks. Depending on storage conditions, lowering the temperature of wine can increase wine oxygenation because oxygen solubility increases in wine at lower temperatures.<sup>9</sup> Comparing various cold stabilization

temperatures on organoleptic quality, it was found that chilling wine to -5 to 0°C followed by a cream of tartar powder addition was the best approach to treat young wines.<sup>10</sup> During crystallization other compounds can coprecipitate with the potassium bitartrate including anthocyanin color compounds.<sup>11</sup> Shorter treatment times may minimize the overall impact of cold stabilization on wine composition.

#### **1.4. Fluidized Beds**

A technology exists that can potentially transform the practice of cold stabilization from a batch process to a continuous process: the fluidized bed crystallizer, shown schematically in Figure 2. A fluidized bed consists of a column of loose particles suspended in an upward-flowing liquid or gas. Fluidized beds are used in industrial applications where the mixing and interaction of fluid and solid media are required, such as catalytic conversions of petroleum gas streams.<sup>12</sup> In a fluidized bed crystallizer the solid media are crystals which act to selectively precipitate the desired ions from solution.

Fluidized beds were demonstrated to be able to remove potassium bitartrate on a bench scale since the 1990's, but so far have not been shown to be used in commercial winemaking.<sup>13</sup> This section explains what fluidized beds are and how this technology can improve the way wineries perform cold stabilization.

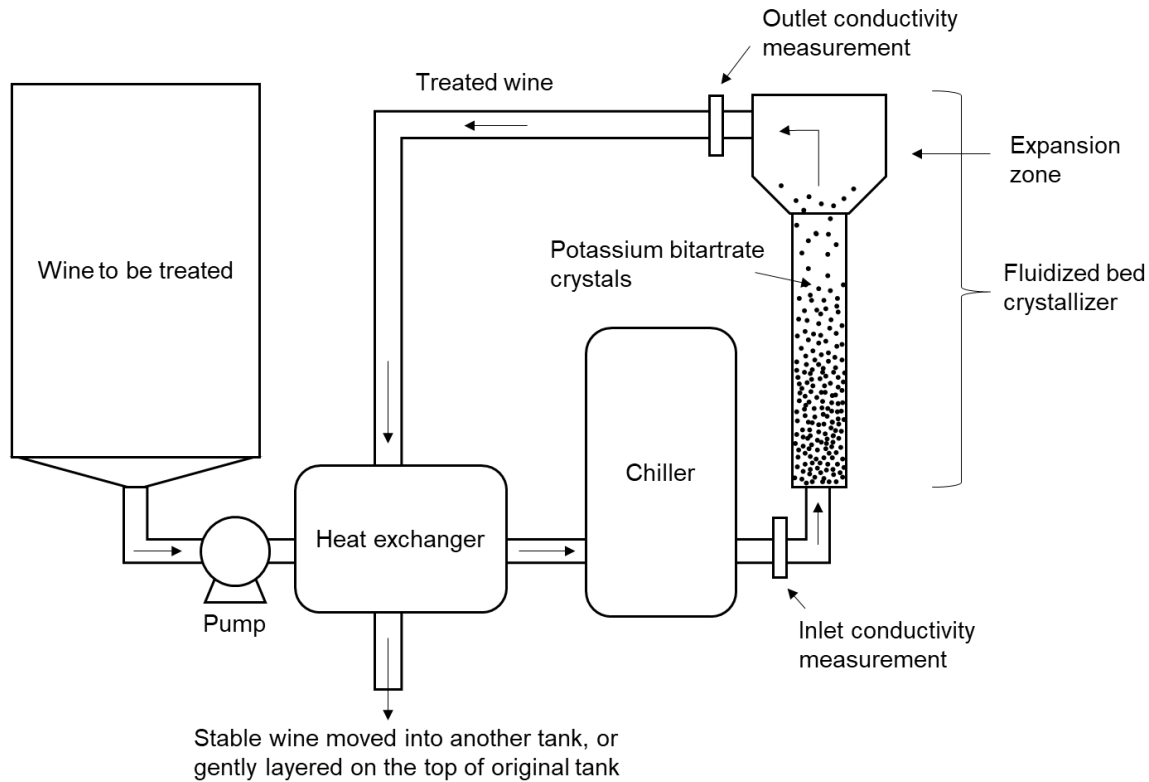


**Figure 2.** Schematic of a fluidized bed crystallizer for wine cold stabilization. Wine is chilled and pumped upwards through a column containing potassium bitartrate crystals, which remove potassium bitartrate in the wine. The treated wine passes through a heat exchanger on the way out, pre-chilling the incoming wine and reducing load on the chiller.

To stabilize wine in a fluidized bed, the temperature of unstable wine is quickly dropped to cold stabilization temperatures using a chiller. The chilled wine is pumped upward in a well-insulated column with loose potassium bitartrate crystals, which act as crystallization nucleation sites. The upward flow of wine lifts the bed of crystals, which are retained within the column by the balancing force of gravity exerted on the particles. The treated wine is passed back through a heat exchanger and exchanges heat with the incoming wine, minimizing the total amount of refrigeration required.<sup>14</sup> Another benefit of this method is that crystallization is isolated in a designated column that can be drained rather than in a large tank where crystals adhere to the sides or settle at the bottom contributing to wine loss. Gently laying treated wine on top of the original tank could possibly save an additional tank to be used altogether.<sup>14</sup>

The upwards flow of wine mixes the crystals and prevents blockage of the column. The crystals continue to grow as potassium and bitartrate are deposited. Pressure sensors across the column can be used to monitor the crystals in the column and control the wine flow rate. A packed bed column is not suitable for crystallization because crystal growth eventually will form an impassable mass blocking liquid flow. Once the treatment is complete, the crystals in the column may be recovered, crushed, and reused as seed crystals for another stabilization treatment or sold as a precursor for cream of tartar.<sup>8</sup> A cycle is created in which the byproducts of stabilization can aid in stabilizing more wine, rather than be disposed.

The concentration of dissolved salts in a solution can be measured by conductivity. Conductivity probes, before and after the fluidized bed can help estimate the amount of potassium bitartrate removed from the wine during the process. Potassium bitartrate stabilization tests such as the rapid conductivity test can guide wineries on how much drop in conductivity is needed to achieve stabilization.<sup>15</sup> Temperature, mass of crystals, and flow rate can be adjusted to reach the correct stability. The fluidized bed can be adapted for different scenarios by adding additional columns. Modular columns will allow seamless transition from one column to another in case a column needs to be switched out.

### **1.5. Electrodialysis**

Electrodialysis, used in desalination applications, is approved for use in removing potassium bitartrate from wine.<sup>16</sup> Wine is passed through a stack of ion-exchange membranes between electrical charges, shown in Figure 3. Positively charged potassium ions ( $K^+$ ) in wine migrate toward the negative electrode and negatively charged bitartrate ( $C_4H_5O_6^-$ ) is drawn toward the positive electrode. The potassium and bitartrate are able to pass through selective membranes and are extracted in a stream of water.

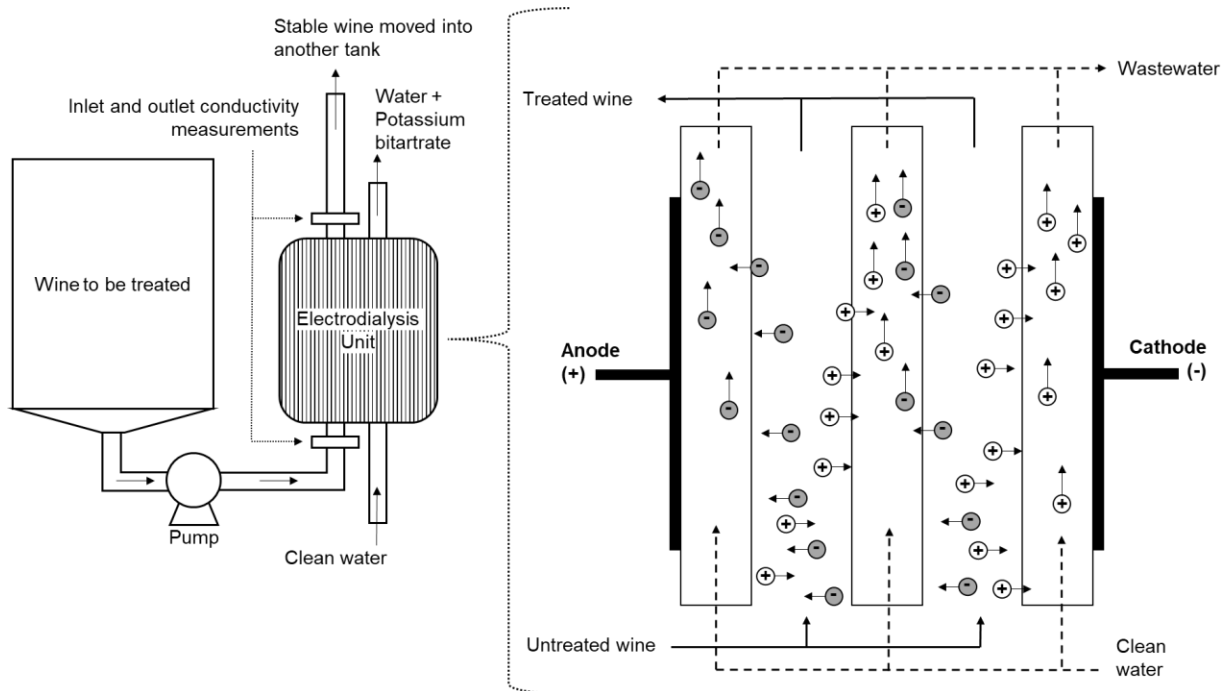


**Figure 3.** Schematic of electrodiagnosis. Wine is pumped through membranes between channels of water. Electrodes on either side create an electric potential difference. Charged ions move through membranes and into a wastewater stream.

Capital cost of electrolysis is likely a deterrent for adopting this technology, but the savings in energy provide an incentive. A study by a California electrical utility company reported that electrodiagnosis reduced the electrical energy consumption by nearly 99% compared to batch cold stabilization.<sup>5</sup> Early adoption of electrodiagnosis showed more water use than cold stabilization, however using reverse osmosis to recycle wastewater has shown promise to decrease water demands.<sup>17</sup> At this point there has been no recovery of potassium bitartrate from this process, unlike cold stabilization and fluidized beds, which can concentrate the potassium bitartrate as a byproduct. To remove the barrier of cost from wineries individually owning an electrodiagnosis unit, some companies offer mobile electrodiagnosis assistance and rent on a per gallon of wine treated basis.

## 1.6. Ion-Exchange

Ion-exchange is used in food, beverage, chemical, and pharmaceutical industries to purify water or isolate valuable products. A common household application of ion-exchange is the conversion of hard water to soft water by exchanging calcium and magnesium ions with sodium and hydrogen ions. The same principle of ion-exchange can be used to reduce potassium levels in a wine.<sup>18</sup> In an ion-exchange process, shown in Figure 4, wine is passed through a column of resinous beads, which are coated in hydrogen ions ( $H^+$ ). Potassium ( $K^+$ ) from the wine replaces the hydrogen ions on the beads, lowering the concentration of potassium in the finished wine.

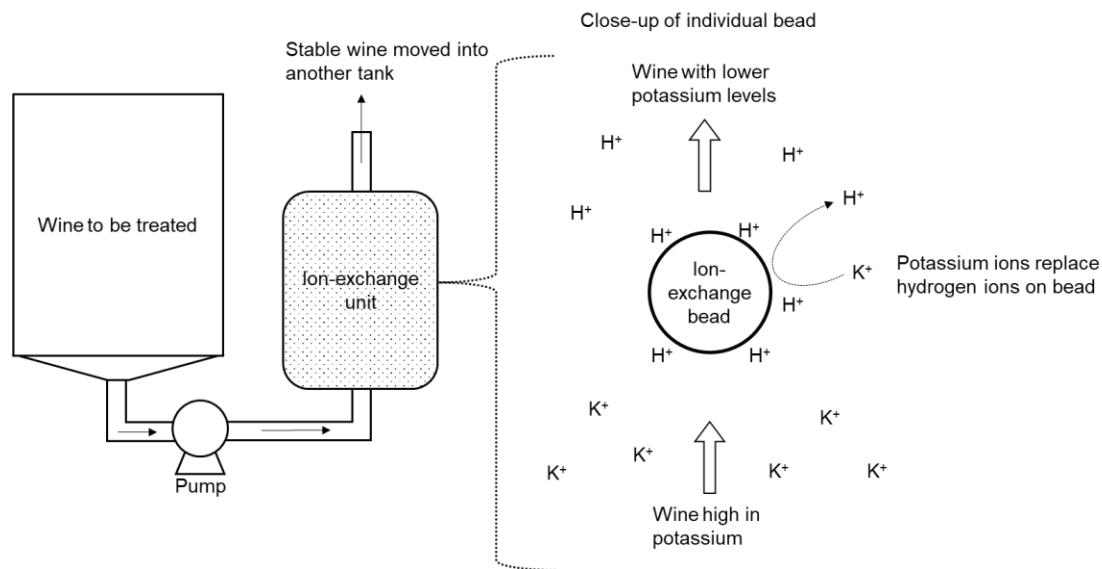


**Figure 4.** Schematic of ion exchanger. Wine is pumped through ion exchange resins which exchange unstable potassium ions ( $K^+$ ) with hydronium ions ( $H^+$ ).

A benefit of ion-exchange is that the wine does not need to be chilled, and stabilization can be achieved in a shorter time than cold stabilization. Besides lowering the wine pH, a disadvantage of ion-exchange is the environmental impact from regenerating the resin beads before stabilizing another batch of wine. The ion-exchange column is flushed typically with a strong acid to replace the potassium with hydrogen again. This process results in a highly acidic waste stream which needs to be properly handled and treated by the winery.

## 1.7. Continuous Bitartrate Stabilization Methods

Some wine-making equipment companies have developed their own proprietary systems to stabilize potassium bitartrate. A continuous bitartrate stabilization method is shown schematically in Figure 5.<sup>19</sup> A scraped-surface heat exchanger chills the wine and scrapes off developing crystals by rotating blades. If a wine is especially high in colloids and difficult to stabilize, metered additions of potassium bitartrate can be added in a mixing tank before the cooler. The chilled wine and crystals are transported to a crystallization tank at 23 °F (-5 °C) where the crystals continue to grow. This is a lower temperature than typical cold stabilization. After the wine reaches stability, it is passed through a filtration system and is ready for bottling. A plate heat exchanger is added for energy recovery. Because of lack of published data on this method it is difficult to compare efficacy with other systems.

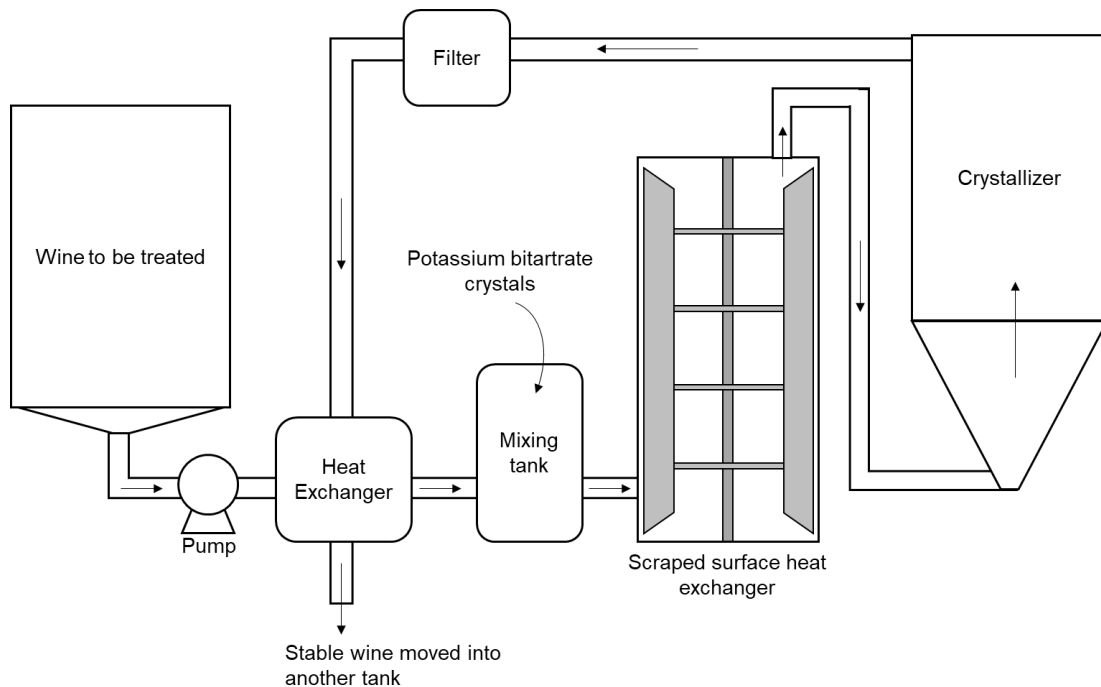


**Figure 5.** Schematic of a continuous crystallization system. Wine is pumped through a mixing tank with metered additions of cream of tartar, chilled in a scraped surface heat exchanger, and flowed upwards in a crystallization tank before being filtered.



## **1.8. Additives for Stabilization**

The list of additives approved for stabilizing potassium bitartrate in wine has expanded in the last two decades. Additives require little-to-no energy or water and minimal labor and treatment time. Although additives offer benefits, a producer may not want to add chemicals to their wine. Perception of taste may be altered and distract from the natural product. There is also the possibility of additives breaking down over time which can leave the wine susceptible to crystallizing after bottling.

### **1.8.1 Carboxymethyl Cellulose**

Carboxymethyl cellulose (CMC) is an ingredient used in many foods and consumer products including ice cream, toothpaste, and bakery goods. CMC is used as a thickening agent to increase viscosity and to stabilize emulsions. CMC is not a natural product but is derived from wood pulp cellulose. Cellulose polymers are broken down and negatively charged carboxy methyl groups are added, which allows CMC to dissolve in water and wine. CMC is used in wine to stop the growth of crystals of potassium bitartrate. The CMC binds to the nucleating crystal and changes the structure, halting growth.<sup>20</sup>

Certain wines should not be treated with CMC. CMC will bind to color tannins and precipitate color compounds out of solution, so it is not advised or approved to use on red wines.<sup>21</sup> All protein fining must be done prior to adding CMC, because CMC can bind to protein and create a haze.<sup>22</sup> CMC may take up to three days to fully dissolve in wine. Because of the viscous nature of this compound, filtering a wine after CMC addition may be problematic.

### **1.8.2 Metatartaric Acid**

Metatartaric acid is formed through an esterification process by heating tartaric acid. The chemical structure is similar to bitartrate so it can bind on the surface of developing crystals and

stop further growth.<sup>23</sup> However, a major downside is that metatartaric acid can reversibly react back to tartaric acid and the wine will become unstable again. All wines treated with metatartaric acid in one study lost their stability in a year, with higher temperatures greatly reducing the lifespan.<sup>24</sup> Therefore, metatartaric acid is useful for wines that will be consumed young and not at risk of exposure to high temperatures. A benefit of this compound is that there seems to be no effect on color stability or creation of a protein haze.

### **1.8.3 Yeast Mannoproteins**

Wines aged longer on yeast were noted to have better tartrate stability. Glycosylated proteins from the yeast cell wall were found to have significant impact on wine cold stability and have since been isolated and approved for this purpose.<sup>25</sup> Yeast mannoproteins are proteins that are coated with mannose sugar molecules and can vary in molecular weight and size. Commercially, these proteins are separated from dead yeast and sold as a beige powder or in liquid form.

The proteins help by coating developing tartrate crystals to stop continued growth of visible precipitates. They are as effective as metatartaric acid and remain effective longer in wine. Yeast mannoproteins aid in reducing the astringency of tannins and increase the smoothness of red wines; however, in some cases the additions resulted in a loss of color.<sup>26</sup>

### **1.8.4 Potassium Polyaspartate**

A recently approved additive for stabilization is potassium polyaspartate, a naturally occurring amino acid salt. Polyaspartate is non-aromatic, with no reported effect on the organoleptic profile of the wine. Potassium polyaspartate lifetime efficacy is impacted by temperature more than carboxymethyl cellulose and discretion should be used if there is a chance the wine will be transported in high temperatures.<sup>27</sup> Polyaspartate is a relatively small molecule and does not change the viscosity of the wine, so poses low risk of clogging membrane filters, unlike other additives.<sup>24</sup>

## **1.9. Summary**

Wine producers aim to decrease energy consumption, water usage, and product loss. Cold stabilization has a large energy demand and relies on hot water and chemicals to clean crystal deposits. New technological advancements in electrodialysis and ion exchange will help enable more efficient stabilization treatment for potassium bitartrate. Fluidized bed crystallizers offer a possibility to replicate cold stabilization in a flow-through continuous process while reducing energy and water usage and minimizing wine loss. New advancements offer on-demand bitartrate stabilization with lower energy expenditure. In some cases, additives may be a preferred option for their low capital cost and ease of use. As factors evolve over the upcoming decades, more wineries may adopt these practices, leading potassium bitartrate stabilization to become less of an economic and environmental problem.

## **Chapter 2. An Investigation of the Hydrodynamic Behavior of Potassium Bitartrate Crystals in Model Fluidized Beds**

### **2.1. Overview**

Fluidized bed crystallizers have been proposed to remove potassium bitartrate in wine, improving upon the typical batch treatment process. Currently, the fluidization of potassium bitartrate crystals is not well understood. In this work we uncover the relationship of the potassium bitartrate crystals to parameters that can be used to model fluidized bed expansion. Potassium bitartrate crystals were made and sieved in sizes from 100 to 2000  $\mu\text{m}$ . Two laboratory-scale fluidized beds were constructed with internal column diameters of 2 cm and 5.1 cm. The columns were loaded with various masses of crystals and bed expansion was measured at different flow rates of a model wine solution. Expansion was dependent on flow rate and crystal size and was independent of mass loading and bed diameter. An empirical model was developed that correlates the parameters that are useful in modeling a fluidized bed crystallizer for this purpose.

### **2.2. Introduction**

Knowledge of the hydrodynamic behavior for a process involving solids and fluids is important in the design and scale-up of the operation. In this chapter, the fluidization of potassium bitartrate crystals in a model wine solution is examined in two laboratory-scale fluidized beds. This information can assist in the design of an industrial-scale fluidized bed for removing potassium bitartrate crystals from wine.

To increase the rate of crystallization, it is common for winemakers to add powdered potassium bitartrate to the top of chilled wine tanks. The added crystals negate the rate-limiting nucleation stage and provide a surface for further crystal growth. To transfer this principle to a

fluidized bed, potassium bitartrate crystals can be placed in a column and chilled wine can be flowed upwards through the crystals, mixing them and the wine, and improving mass transfer. The flow expands the bed of crystals but does not transfer the crystals away. Supersaturated potassium bitartrate in the chilled wine deposits onto the crystals. As the crystals grow the fluidized nature of the particles allows them to mix and not form a blockage. When the treatment is done, the crystals can be removed, crushed and reused again to treat another wine.<sup>8</sup>

Although the concept has been explored in a laboratory, there have been no tests done on a pilot or industrial scale, particularly due to the lack of knowledge on how the crystals will behave under different flow conditions. A primary factor limiting the study of fluidized beds for this purpose is the lack of potassium bitartrate crystals available on the market, although this thesis work has prompted suppliers to remedy this need. Currently potassium bitartrate is sold as a finely pulverized powder, known commonly as the baking ingredient, cream of tartar. The powdered form is preferred for maximizing the surface area to mass ratio on which crystals can grow. However, the finely ground powder is easily carried away at flow rates required to sustain a fluidized bed. It is possible to create larger crystals, for instance by dissolving the powder in warm water and then cooling to facilitate crystal formation. By testing the fluid dynamics of different crystal sizes, one can better estimate the hydrodynamic behavior and extrapolate to design an industrial-scale fluidized bed reactor.

Fluidized beds are a common unit operation in chemical engineering because they facilitate mass transfer with a high surface area between a solid and liquid or gas.<sup>28</sup> The fluidized bed is formed when a fluid passes upward through a column containing a bed of particles. The fluid causes the particles to experience an upward drag force, causing the particle bed to expand. The bed expansion ( $\epsilon$ ), also known as porosity and voidage, is the fraction of space within the bed

which is associated with the fluid phase. As the bed expands, the voidage inside the bed increases, which lowers the fluid velocity in the bed, decreasing the drag on each particle. When the drag forces and weight of the particles are balanced the bed of particles is fluidized.

A useful metric of the fluidized bed in operation is the residence time ( $t_r$ ), which refers to the average time a fluid spends passing through the bed. A higher residence time allows for more potassium and bitartrate ions in solution to transfer to the particles and crystallize. For fluidized beds, the residence time is determined as a function of the bed height ( $h$ ), superficial fluid velocity ( $u_s$ ) and  $\varepsilon$ . The superficial velocity is a function of the flow rate ( $Q$ ) and the diameter of the column ( $D$ ) and represents the average velocity experienced in each cross section of the column.

$$t_r = \frac{h \varepsilon}{u_s} \quad (1)$$

$$u_s = \frac{Q}{\pi \left(\frac{D}{2}\right)^2} \quad (2)$$

The terminal velocity of a falling particle ( $u_t$ ) can be approximated using fluid and particle characteristics, assuming spherical particles.

$$u_t = \frac{(\rho_s - \rho_f) g d_p^2}{3000\mu} \quad (3)$$

The minimum fluidization velocity can be calculated using the measured unexpanded bed voidage ( $\varepsilon_0$ ) and  $u_t$ .

$$u_{mf} = \frac{\varepsilon_0^3 u_t}{8.33(1 - \varepsilon_0)} \quad (4)$$

The following relation can then be used to determine the bed voidage at different values of ( $u_s$ ).

$$\frac{\varepsilon^3}{1 - \varepsilon} = \frac{\varepsilon_0^3}{(1 - \varepsilon_0)} + \frac{8.33(u_s - u_{mf})}{u_t} \quad (5)$$

The Ergun equation is useful in predicting pressured drop,  $\Delta P$ , of packed and fluidized beds over a defined length,  $L$ , with other structural parameters.<sup>29</sup> Because pressure drop and expansion cannot be known directly, a numerical approach is needed to plot the equation.

$$\frac{\Delta P}{L} = \frac{150(1 - \varepsilon)^2}{\varepsilon^3} \frac{\mu u_s}{(\phi d_p)^2} + 1.75 \frac{(1 - \varepsilon)}{\varepsilon^3} \frac{\rho u_s}{\phi d_p} \quad (6)$$

The terminal velocity equation assumes that the particles are spherical and uniform in size. For many applications, this is a useful assumption because the behavior of fluids around a sphere are well studied and predictable. Potassium bitartrate crystals, however, are not spherical due to crystal growth being preferred in some directions more than others. To account for non-spherical particles in fluidized bed models,  $d_p$  is multiplied by the sphericity,  $\phi$ , resulting in the modified particle size ( $D_p$ ).

$$\phi = \frac{SA_{sphere}}{SA_{particle}} \quad (7)$$

$$\phi d_p = D_p \quad (8)$$

The sphericity is a 3D property of a particle, which is difficult to measure directly without a high-resolution 3D scanner. An approximation to this value can be made by squaring the circularity ( $C$ ), a 2D equivalent of the sphericity, which can be measured through optical microscopy.

$$C = \frac{P_{circle}}{P_{particle}} \approx \frac{2\pi r_{circle}}{2\pi r_{particle}} = \sqrt{\frac{4\pi r_{sphere}^2}{4\pi r_{particle}^2}} \approx \sqrt{\frac{SA_{sphere}}{SA_{particle}}} = \sqrt{\phi} \quad (9)$$

This makes aspherical particles behave as smaller particles, which can fluidize easier due to a higher mass to surface area ratio. The terminal velocity calculation can thus be improved by using the modified particle size.

$$u_t = \frac{(\rho_s - \rho_f) g D_p^2}{3000\mu} \quad (10)$$

Additionally, in production the crystals are sifted to select specific crystal sizes, which produces a crystal size distribution rather than a specific crystal size. Studying the effect of the size distribution on the fluidized bed, will improve the predictability, or modeling, of the fluidized bed.

The dimension of a non-circular shape can be described by the maximum Feret diameter ( $F_{max}$ ) and the minimum Feret diameter ( $F_{min}$ ), illustrated in Figure 6. Sometimes referred to as Feret length or caliper length,  $F_{max}$  and  $F_{min}$  refer to the longest and the shortest length that a caliper could measure from a particle.<sup>30</sup>

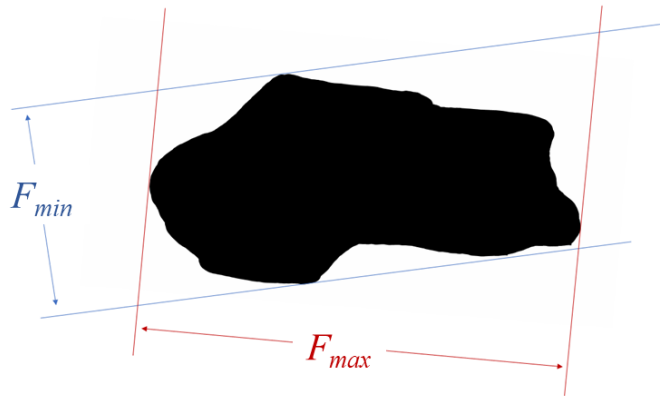


**Figure 6.** Illustration of minimum Feret diameter ( $F_{min}$ ) and maximum Feret diameter ( $F_{max}$ ) for a crystal particle.

## 2.3. Materials and Methods

### 2.3.1 Bench-scale Fluidized Beds

Two model fluidized beds were constructed and are shown in Figure 3. The columns are made of clear PVC tubing with inner diameters of 2 cm and 5.1 cm, and heights of 90 cm and 122 cm, respectively. The columns are capped on each end with a 100  $\mu\text{m}$  wire mesh screen to keep the crystals within the column. A 5000 mL beaker was filled with a model wine solution. The



model wine was drawn out of the container and pumped into the column by a precision peristaltic pump (Masterflex model 1300-3600, Thermo Fisher Scientific, USA) and fitted with Masterflex tubing size 14 and 18, depending on the required flow. After reaching the top of the column the model wine flows in a tube back into the reservoir and is recirculated. A thermometer in the beaker monitors the temperature of the solution.

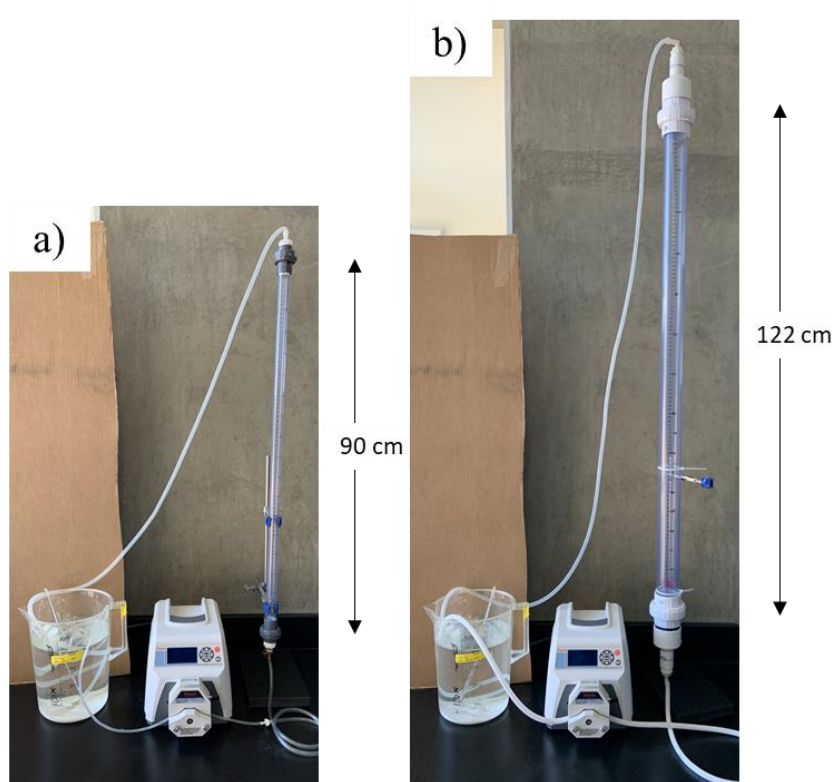


**Figure 7.** Photos of the model fluidized beds with inner diameters 2cm (a) and 5.1cm (b). Model wine in the beaker is pumped through the bottom of the column, raising a bed of crystals, and then returned to the beaker.

### 2.3.2 Potassium Bitartrate Crystals

Potassium bitartrate crystals, used in the study were created in-lab and sieved into fractions before use, shown in Figure 8. Potassium hydrogen tartrate, sold as natural cream of tartar (Tártaros Gonzalo Castelló, Spain) was dissolved in water and held at 30 °C for three days in 50-gallon tanks with constant agitation. The tanks were subsequently chilled to 5 °C for another three days to recrystallize the solubilized potassium bitartrate into larger crystals. The water was flushed, and

crystals were removed from the tank and air dried in a laminar flow hood for three days. Crystals were separated into five fractions from 180  $\mu\text{m}$  to 2000  $\mu\text{m}$  using a Mary Ann® Sieve Sifter (Humboldt, USA) for 30 minutes. The sixth set of crystals, nominally referred to as 100  $\mu\text{m}$ , were specially ordered (Tártaros Gonzalo Castelló, Spain).

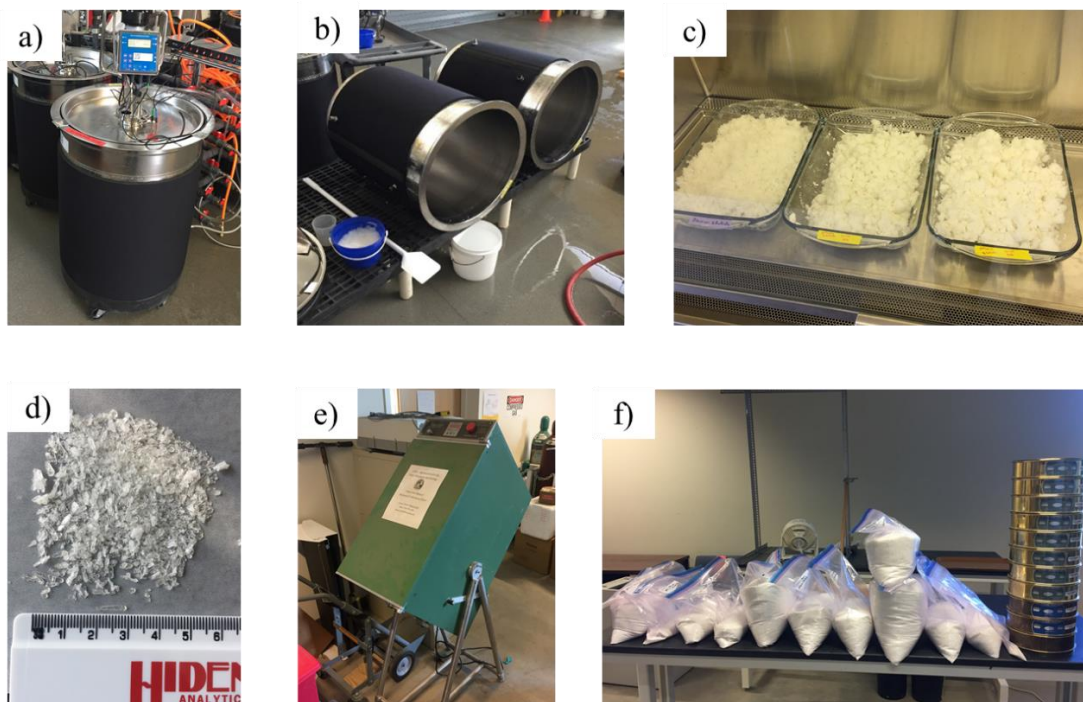


**Figure 8.** Photo gallery of the crystal making process. a) 50-gallon tank used to dissolve and recrystallize powdered potassium bitartrate. b) Crystals being removed from tanks into buckets. c) Crystals drying in a fume hood. d) Dried crystals before sieving. e) The Mary Ann shaker used to separate crystals. f) Final result of sieving crystals into various size fractions.

Instruments at the Advanced Materials Characterization and Testing Laboratory (AMCaT) at UC Davis were used to analyze the particle size of the potassium bitartrate crystals. Images were taken with a PAXcam PX-CM microscope camera (PAX-it, USA) using an Olympus SZX7 stereo microscope (Olympus Optical, Japan). Crystals were placed on a microscope slide and scattered to avoid overlap of crystals. Images were analyzed on ImageJ (Version 1.53k, Nation Institutes of Health) by subtracting the background image, thresholding until the crystals were well defined, and then using the built-in particle analyzer.

### **2.3.3 Model Wine Solution**

A model wine solution, with a concentration of 12% abv, was made by mixing distilled water and 190 proof ethyl alcohol (Koptec, USA). An excess amount of powdered potassium L-tartrate monobasic (Sigma-Aldrich, USA) was added to create a supersaturated solution which would not dissolve the crystals in the column. The temperature of the model wine was room temperature (21°C) and did not change during fluidization, so it is assumed no growth or dissolution of the crystals occurred during the experiment.

### **2.3.4 Measurements**

Potassium bitartrate crystals were weighed using an analytical balance (Denver Instrument, USA) and placed inside the column, contained by 100  $\mu\text{m}$  mesh screens fitted into gaskets at each end. Once loaded with crystals, the column was secured, and the tubing was added. The precision peristaltic pump pumped the model wine from the beaker to the bottom of the column up through the crystals. The flow rate of liquid was controlled by the pump and was calibrated before each experiment.

Flow rates to be studied for each crystal size and loading were determined based on the maximum flow rate for which a bed height could be determined. Once the highest flow rate was chosen, an evenly spaced set of flow rates was determined. The order of flow rates in the experiment was randomized using a number sequence randomizer ([www.random.org](http://www.random.org)). Flows were held constant until the bed height stabilized (i.e., no observable change in bed height for three or more minutes) The bed height was measured to the nearest millimeter. A close-up photo of the crystals fluidized in the 5.1 cm diameter column can be seen in Figure 9. All experimental conditions were studied in triplicate.

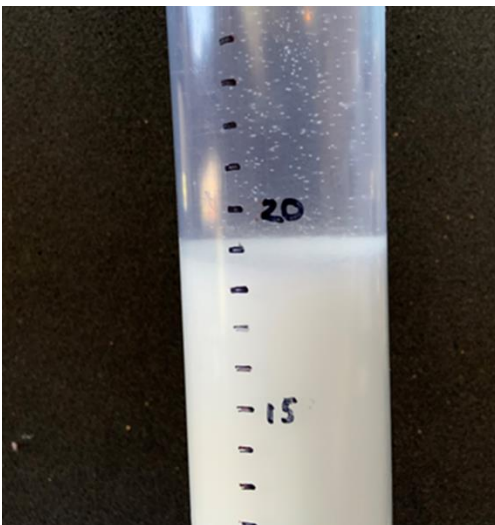


**Figure 9.** Photo of the top of the fluidized bed of crystals in the 5.1 cm diameter column.

After a stable bed height was obtained and the data recorded, the next flow rate was entered into the pump. It took approximately ten minutes for most crystal sizes to reach a stable bed height. The process continued until all targeted flow rates were measured.

## **2.4. Results and Discussion**

### **2.4.1 Particle Analysis**

Before constructing a fluidization model, it was necessary to know the average dimensions of each of the six crystal sizes separated by sieving. An example of each fraction seen under an optical microscope is shown in Figure 10. Additional images of the crystals can be found in the Supplemental Figures section (Figures S1-6). Five samples of crystals for each set were imaged and analyzed. For ease of communication, the crystals throughout this text are referenced by their ‘nominal’ size, which is the mesh size, in microns, that they were retained on, and not the average calculated size.

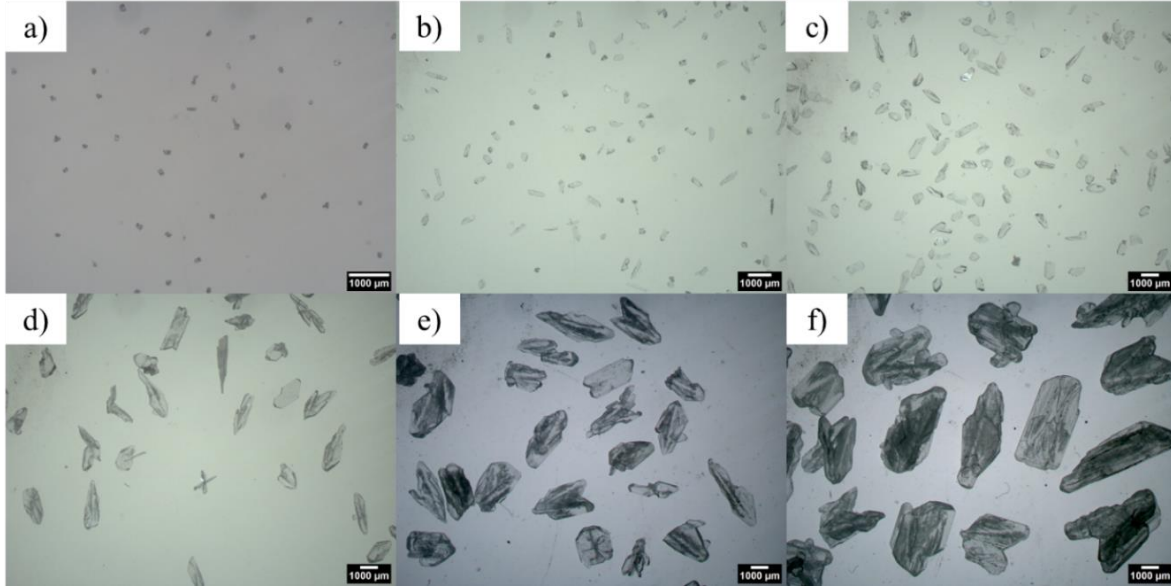


**Figure 10.** Photos of the six crystal fractions studied under an optical microscope. Size refers to the mesh size of the sieve in which the crystals were retained: a) 100  $\mu\text{m}$ . b) 180  $\mu\text{m}$ . c) 355  $\mu\text{m}$ . d) 710  $\mu\text{m}$ . e) 1000  $\mu\text{m}$ . f) 2000  $\mu\text{m}$ .

Parameters analyzed for each set were maximum Ferret, minimum Ferret, and circularity. Sphericity was calculated using the method described in the Introduction. The results of the ImageJ particle analysis were plotted in histograms in Python (Version 3.8, Python Software Foundation) and fit to a normal distribution (Equation 11). The mean and standard deviation values were calculated and are tabulated in Table 1. An example of the histogram and distribution analysis for the 355  $\mu\text{m}$  nominal crystals is shown in Figure 11.

$$f(x) = Ae^{-\frac{(x-\mu)^2}{2\sigma^2}} \quad (11)$$

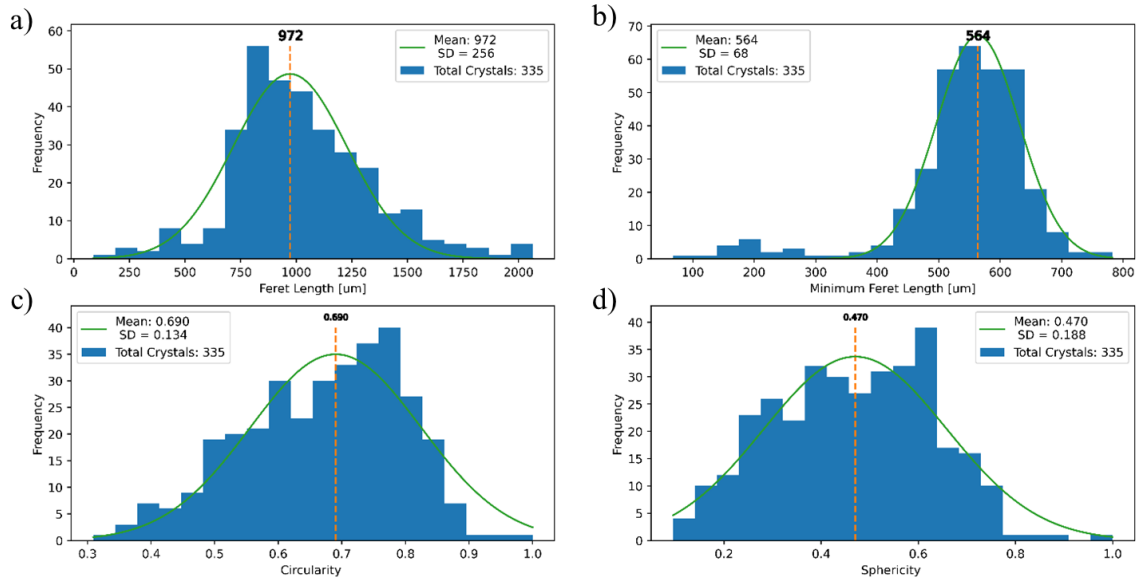


**Figure 11.** Results of particle analysis for crystals captured between a 425  $\mu\text{m}$  and 355  $\mu\text{m}$  sieve. a) maximum Feret length, b) minimum Feret length, c) circularity, and d) sphericity.

**Table 1.** Results of Particle Image Analysis

Nominal Size [ $\mu\text{m}$ ]	Sifting Fraction [ $\mu\text{m}$ ]	Number of Crystals Analyzed	Maximum Feret Length [ $\mu\text{m}$ ]		Minimum Feret Length [ $\mu\text{m}$ ]		Circularity		Sphericity	
			Mean	SD	Mean	SD	Mean	SD	Mean	SD
100	N/A	388	200	36	144	21	0.77	0.084	0.587	0.133
180	180 - 212	356	508	165	283	34	0.719	0.169	0.492	0.247
355	355 - 425	335	972	256	564	68	0.69	0.134	0.47	0.188
710	710 - 850	137	1625	268	990	136	0.704	0.221	0.422	0.281
1000	1000 - 1700	107	3369	847	1599	306	0.541	0.116	0.279	0.129
2000	2000 - 2800	89	4524	571	2753	306	0.576	0.09	0.323	0.099

For all nominal crystal sizes, both maximum and minimum mean length determined by image analysis was larger than the retaining sieve size, which was expected. The crystals tend to become more elongated and less circular as they increase in size. The mean circularity of the smallest crystals (100  $\mu\text{m}$ ) was  $0.77 \pm 0.084$ . The largest crystals (2000  $\mu\text{m}$ ) mean circularity was  $0.576 \pm 0.09$ , which amounts to a 33.7% decrease in circularity compared to the smallest crystals.

The mean sizes and sphericities for these particles were used in the following assessment of the fluidization results.

### 2.4.2 Fluidization Analysis

The complete set of data points collected in this study are shown in Figure 12 with each color representing a data point from a certain size crystal set. Bed voidage is a measure of the space between the particles in the bed. Smaller particles fluidize easily and increase bed voidage at low flows whereas larger particles require higher velocity to expand a similar amount.

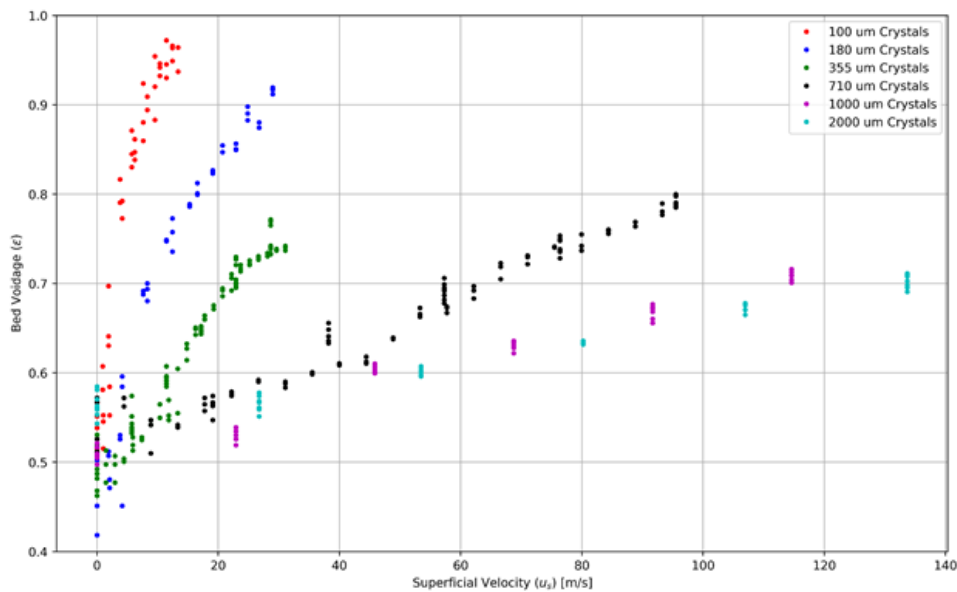


**Figure 12.** Bed voidage vs. superficial velocity for the six crystal sizes studied. Data set contains all points, with varying bed masses and from both columns included.

To understand which variables are most important in modeling bed voidage for scale-up, experiments were performed by varying mass of crystals loaded and the diameters of the columns. Figure 13 shows the impact of increasing masses loaded into the smaller column. Three loading masses were chosen: 15 g, 30 g, and 60 g. All data, represented by different color markers for each crystal size, lie on the same line. This result indicates that similarly sized crystals expand the same for a given flowrate regardless of the mass added.

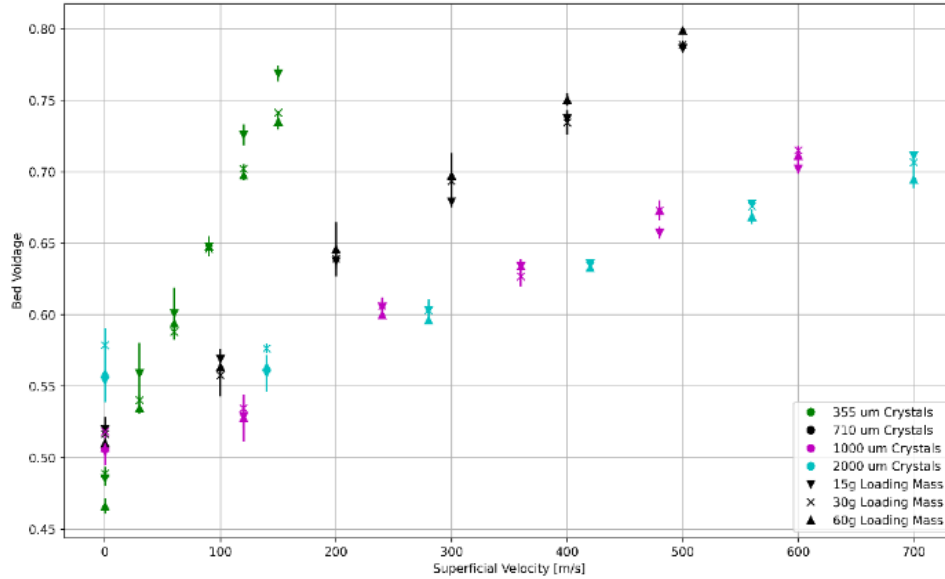


**Figure 13.** Plot of bed voidage vs. superficial velocity for four crystal sizes with three varying masses of crystals added. ▼= 15 g, X= 30 g, ▲= 60 g

Likewise, Figure 14 shows the results of testing bed expansion in two different diameter columns, 2 cm and 5.1 cm, indicated by down and up arrows, respectively. The colored markers lie on the same line for all crystal sizes, without a noticeable trend for one column size to another. These results suggest that tests on a small-scale column can be interpreted for a larger column.

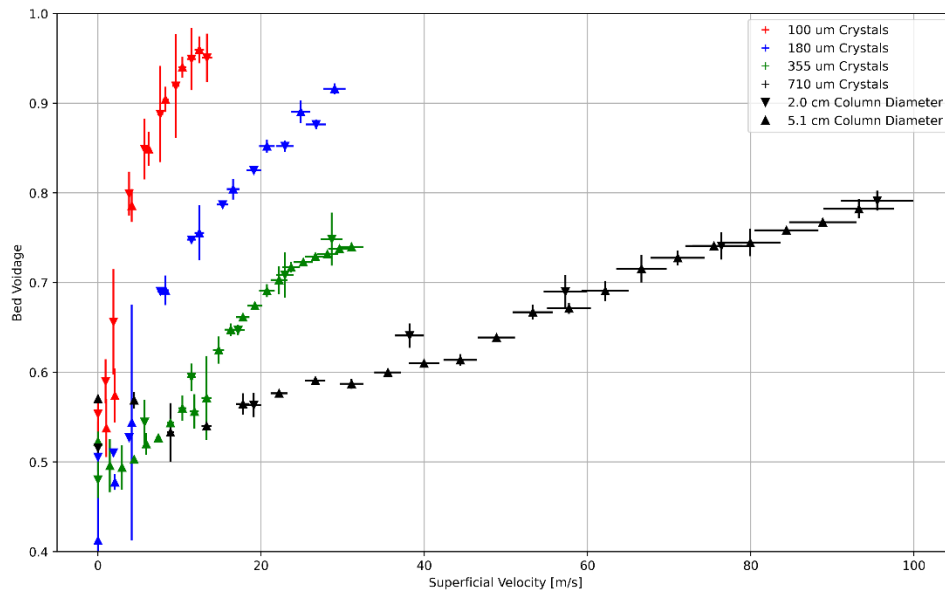


**Figure 14.** Bed voidage vs. superficial velocity for four crystal sizes in the two columns.



▼ = 2 cm diameter, ▲ = 5.1 cm diameter

The Reynolds number is a dimensionless number indicative of inertial forces versus viscous forces; in this experiment we are focused on the Reynolds number of the crystal particle (Equation 12).<sup>31</sup>

$$Re_p = \frac{u_s d_p}{\nu} \quad (12)$$

The calculated Reynolds number for the six crystal sizes versus superficial velocity is shown in Figure 15. Reynolds number of larger crystals increase faster than smaller particles with increasing superficial velocity. Figure 16 displays the experimental data for bed expansion versus Reynolds number for the particles. Plotting non-dimensional data shows little effect from tube size and mass loading but a strong correlation with particle size. A bench-scale column will therefore likely be able to extend results to a larger commercial-scale fluidized bed given that the same sized crystals are used.

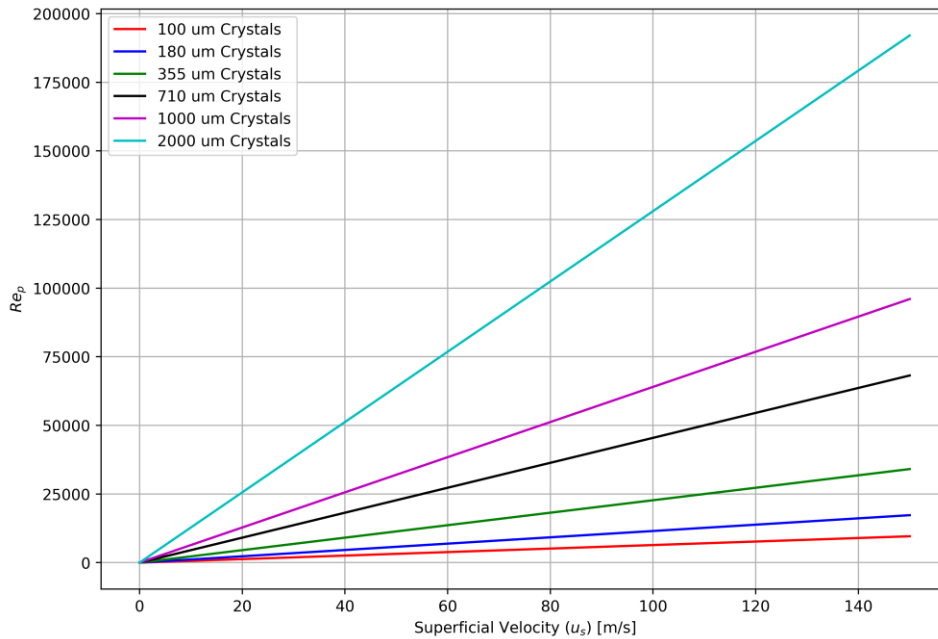


**Figure 15.** Calculated particle Reynolds number for each of the six crystal sizes vs. superficial velocity.

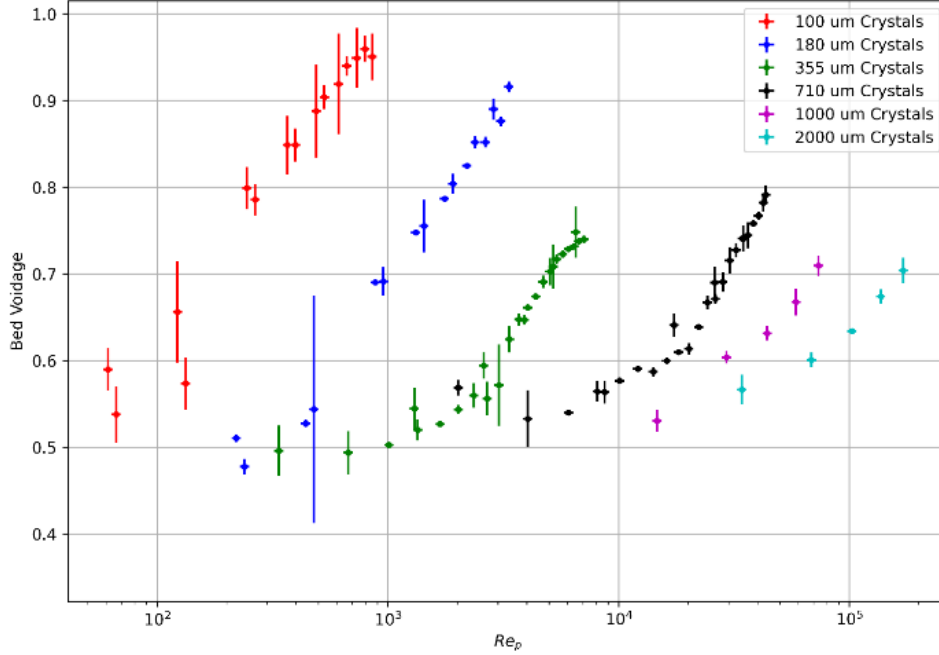


**Figure 16.** Bed voidage vs. particle Reynolds number for the six crystal sizes.

The next step was to determine an equation that could be used to predict bed expansion using an empirically driven voidage prediction polynomial.<sup>32</sup> The two most important variables were crystal size and flow rate, so a power equation was fit using these two parameters. The resulting equation had the form shown in Equation 13 with variable coefficients shown in Table 2. This equation considers the modified particle size and superficial velocity. The modified particle equation combines information from sphericity and particle length to better fit the data. The polynomial fit equation using a least squares fitting algorithm is plotted as solid lines in Figure 17. The Ergun equation (Equation 6) is plotted in dashes along with the data points collected.

$$\varepsilon = \sum_{i,j} C_{i,j} D_p^i u_s^j \quad (13)$$

**Table 2.** Coefficients for the 16-term 2D power series fit for fluidization data.

	$u_s^0$	$u_s^1$	$u_s^2$	$u_s^3$
$D_p^{-2}$	-0.0570	-3.28	-47.7	0.238
$D_p^{-1}$	10.8	9.29	0.0733	-5.04E-4
$D_p^0$	0.400	-0.00989	-5.83E-05	4.86E-07
$D_p^1$	9.98E-05	2.03E-06	3.81E-08	-2.42E-10

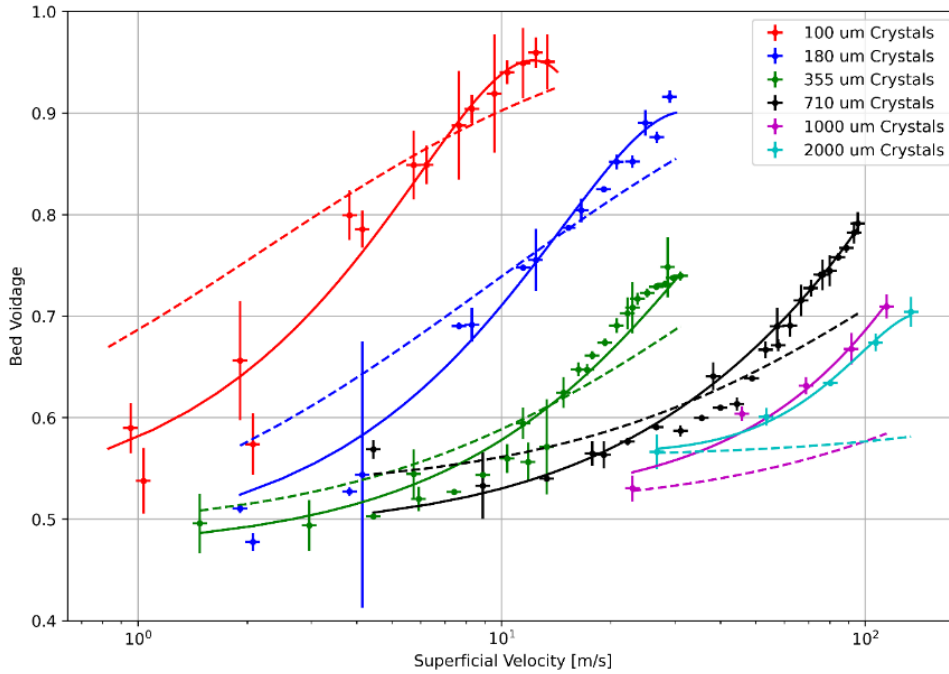


**Figure 17.** Bed voidage vs. logarithmic superficial velocity overlaid with the best-fit power function (solid line) and modified Ergun model (dashed).

With the polynomial fit equation, we can model the residence time as a function of the superficial velocity in the column and the particle size, shown in Figure 18. This can be helpful in predicting how long a fluid will pass through the column given known parameters. The vertical dashed lines are the equation's best predictions of the minimum fluidization velocity needed to fluidize the bed, given the crystal size. The data for all crystal sizes follow a diagonal line until they reach their respective minimum fluidization, wherein they begin to diverge from the line.

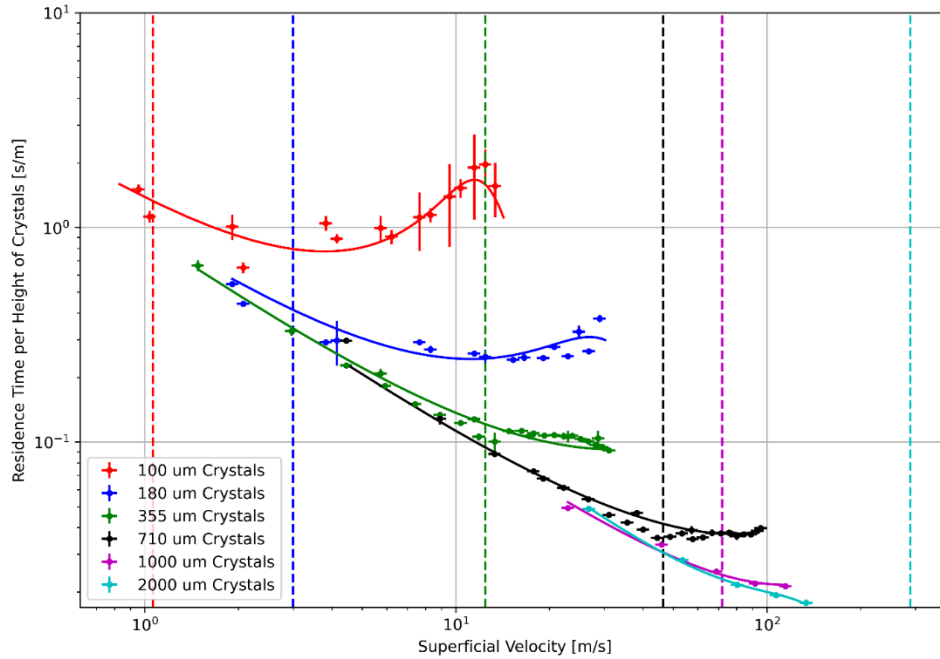


**Figure 18.** Residence time vs. velocity. Solid line is the best-fit power equation, dashed lines designate minimum fluidization velocity.

## 2.5. Summary

This study is a first look into the fluid dynamics for the use of potassium bitartrate crystals in a fluidized bed crystallizer that is operating with a model wine solution. The main factor used in predicting bed expansion was found to be particle size and fluid velocity. The estimate improved further using the sphericity of the particle to modify the particle diameter. Tube diameter and loading amount did not show a noticeable effect on bed expansion. Using two variables, the superficial velocity ( $u_s$ ) and the modified diameter ( $D_p$ ) a polynomial equation was found to cover a wide range of crystal sizes (100 – 2000  $\mu\text{m}$ ) and can be used to predict bed expansion in a fluidized bed.

## **Chapter 3. The Removal of Potassium Bitartrate in a Pilot-scale Fluidized Bed Crystallizer**

### **3.1. Overview**

A pilot-scale fluidized bed crystallizer was designed, constructed, and tested for removing potassium bitartrate from a wine. Conductivity measurements before and after the column showed a decrease in conductive ions, indicating that crystallization occurred in the column. Measurements of six organic acids before and during the experiment confirm there was a decrease in tartaric acid and no effect on other organic acids present. Particle analysis of the crystals before and after use in treatment confirm that the seed crystals increased in size. This work provides proof-of-concept and evidence that with further experimentation and development this process could one day achieve wine stabilization on an industrial scale.

### **3.2. Introduction**

#### **3.2.1 Crystallization**

Prior work has demonstrated crystallization reactions occur in a two-step process, a nucleation stage and a growth stage.<sup>33</sup> Crystallization is driven by the disparity between a supersaturated solution and the saturation point. It has been demonstrated that potassium bitartrate crystallization is rate limited in the nucleation stage.<sup>34</sup> Cold stabilization achieves stabilization by reducing the temperature of a wine, thus decreasing the solubility and facilitating crystal growth. After days of chilling in a tank, the wine contains less ions in solution and is removed from the crystals. Cream of tartar (potassium bitartrate powder) can be added increase the rate of crystallization, through elimination of the nucleation stage. Such crystallization is referred to as batch cold stabilization because the entire tank is treated in a singular batch.

The fluidized bed crystallizer works by containing a potassium bitartrate crystals in a column and flowing chilled wine through them, rather than adding crystal powder to a tank. This approach will increase the interaction between the wine and seed crystals, which enables faster stabilization, and keep the potassium bitartrate in a column rather than the sides and bottom of a tank.

### **3.2.1 HPLC**

Wine is a complex chemical mixture derived from the pressing and fermentation of grapes, lending to characteristic flavors and smells. Besides the main components of water and ethanol, wine contains hundreds of identifiable compounds in categories such as carbohydrates, acids, proteins, phenolics, and esters.<sup>35</sup> In order to determine if the target molecule, potassium bitartrate, was removed during the experiment, chromatography was used to differentiate the major organic acids in the wine at various time points. High performance liquid chromatography (HPLC) is a type of chromatography that can be used to separate and detect molecules in a liquid solution. An unknown mixture is passed through a column with selectivity for a certain chemical property. A metered addition of a mobile phase removes the molecules from the column slowly, so that they can be separated and quantified by a spectrophotometer.

## **3.3. Materials and Methods**

### **3.3.1 The Development of a Pilot-scale Fluidized Bed Crystallizer**

A pilot-scale fluidized bed crystallizer was fabricated at the Beringer Winery in St. Helena, CA shown in Figure 19a. The crystallizer was built on a movable platform which allows the unit to be maneuvered around the winery and service specific tanks that need bitartrate stabilization. Along with the unit is a movable tube-in-tube chiller (Kreyer model SR-17, Föhren, Germany) to chill the wine before it enters the column of crystals (Figure 19b). Both the unit and

chiller run on 480-volt 3-phase power. The use of the chiller in this experiment was a result of availability, and not from sizing calculations or specifications.



**Figure 19.** Photos of the completed fluidized bed system. a) The pilot-scale fluidized bed unit at the UC Davis research winery. b) Chiller used to chill incoming wine. c) Touch screen control panel.

A PLC cabinet is mounted on the unit that houses the electronics and a user interface panel (Figure 19c). The information panel contains a touch screen monitor connected to an onboard computer that runs Windows 10. Ignition software (Inductive Automation, Folsom, California) is used to compile data from sensors throughout the system. A user is able to modify the pump speed, monitor real-time and historic data stored on the computer and turn on an LED light strip in the column to view inside. Two external USB ports allow a computer mouse and flash drive to access the computer without opening the electrical cabinet.



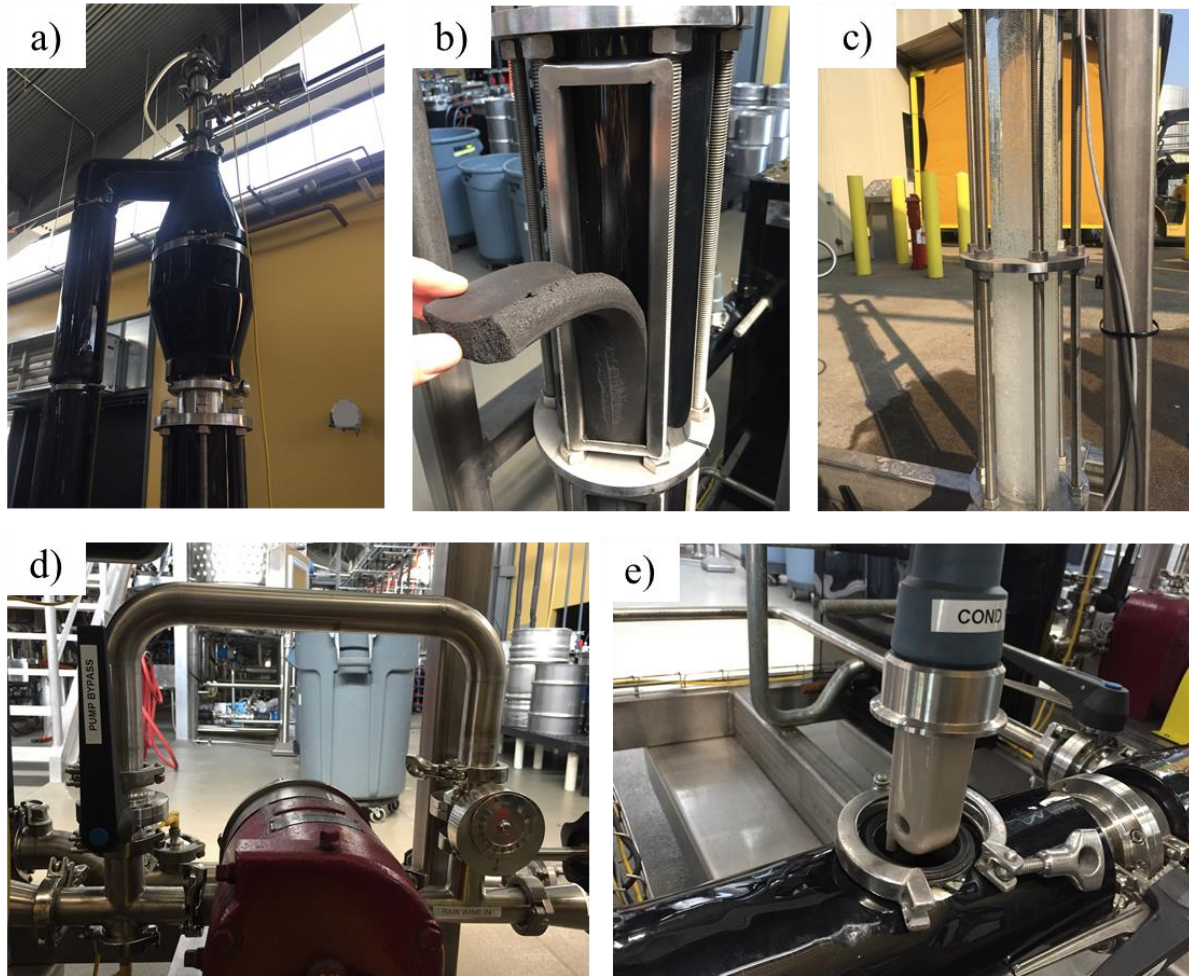


**Figure 20.** Photos of components of the fluidized bed system. a) Disengagement zone at the top of the column to reduce fluid velocity. b) Removable foam for viewing the column c) Glass column with fluidized crystals before insulation was added. d) Pump bypass to achieve lower flow rates. e) Endress + Hauser inductive conductivity probe fit inside the piping with a Tri-Clover clamp.

A rotary lobe pump is used to move the wine throughout the system using positive displacement. The pump was oversized for the low flow rates necessary for this experiment, so a recirculating loop was put into place to reduce the flow to the column (Figure 20d). An electromagnetic flow meter (Promag 300, Endress+Hauser, Switzerland) measures the flow rate of wine passing through the unit. A plate and frame heat exchanger with 31.63 square feet of surface area provides energy recapture by chilling incoming wine with outgoing wine (Alfa Laval,



Sweden). Additional information on the heat exchanger can be found in the Supplemental Figures section (Figure S7).

The glass column containing the crystals is five feet in length with an internal diameter of four inches. A photo of the column with fluidized crystals, before insulation was added, is shown in Figure 20c. The column and most of the pipe work is covered in insulation to prevent heat transfer with the outside air. Removable foam blocks are installed along the column, for visualization of the fluidized crystals when necessary (Figure 20b). At the top of the column is an expansion chamber with an inner diameter of eight inches which reduces the velocity of the upward flow and helps prevent smaller particles from exiting the column (Figure 20a). 100  $\mu\text{m}$  screens are placed before the column and after the expansion chamber to hold the crystals in place during operation. Crystals are removed from the bottom of the column by separable Tri-clover clamps.

Temperature, pressure, and conductivity are measured at the inlet and outlet of the column. Temperature and conductivity are measured using an inductive conductivity meter (Indumax CLS54D, Endress+Hauser, Switzerland) connected to a universal four-wire multichannel controller (Liquiline CM444, Endress+Hauser, Switzerland). Pressure transducers before and after the column are a safety measure that enables the pump to be stopped if a pressure differential reaches a set point.

### **3.3.2 HPLC**

HPLC was used to differentiate and quantify the organic acids in wine sampled before and during the test of the pilot-scale crystallizer experiment. Six organic acids commonly found in wine were analyzed: tartaric, malic, acetic, lactic, citric, and succinic. Analysis was performed by an Agilent HPLC system (1100 series, Agilent Technologies, Santa Clara, California) using a Kinetex F5 2.6  $\mu\text{m}$  Core-Shell HPLC Column. The mobile phase was 20 mM potassium

dihydrogen phosphate ( $\text{KH}_2\text{PO}_4$ ). Samples of wine were centrifuged at 5000 rpm for 5 minutes, filtered with a 0.45  $\mu\text{m}$  Nylon syringe filter, and diluted 10 times with mobile phase. Each sample was prepared in triplicate. A standard curve was made with known concentrations of organic acids to convert area to concentration. Python was used to process the spectrophotometric data obtained through HPLC.

### **3.3.3 Particle analysis**

Particle analysis of crystal shape and size before and after the experiment was determined using the method detailed in Chapter 2.

### **3.3.4 Potassium Bitartrate Stability**

Potassium bitartrate stability was determined using a Check Stab instrument (Delta Acque di A. Cavallucci, Florence, Italy). This instrument chills a wine to 30 °F (-1.1 °C) using a glycol bath and then adds 1 gram of cream of tartar powder to initiate rapid crystallization of potassium bitartrate. A conductivity probe in the wine measures the change of electrical conductivity. The percent change of conductivity provides a basis for how unstable the potassium bitartrate is in the wine. Generally, if a wine shows a decrease in conductivity less than 5%, it can be considered stable.<sup>36</sup>

### **3.3.5. Experimental Procedure**

A white wine at the Beringer Winery was chosen that exhibited a high level of potassium bitartrate instability: an 18% decrease in conductivity determined by Check Stab. The fluidized bed unit was sanitized and rinsed with water. Based on fluidization calculations determined from data in Chapter 2, the column was filled with 2000 g of potassium bitartrate crystals (nominal size 100  $\mu\text{m}$ , Gonzalo Castello, Spain). Wine was pumped from the tank through a heat exchanger, through the chiller, through the column of crystals, and then back through the

heat exchanger to pre-chill incoming wine. Conductivity, temperature, pressure, and flow rate data was captured and are presented below. The experiment lasted 4 hours.

### 3.4. Results and Discussion

The conductivity measurements before and after the fluidized bed column are shown in Figure 21. Time zero refers to the moment at which the valve to the column was opened and chilled wine was allowed to enter and fluidize the crystals. After some fluctuations, a steady differential of conductivity is observed. Throughout most of the 4 hours of the experiment there was a conductivity drop of  $100 \mu\text{S}/\text{cm}$  (14.3%) from the infeed to the outfeed.

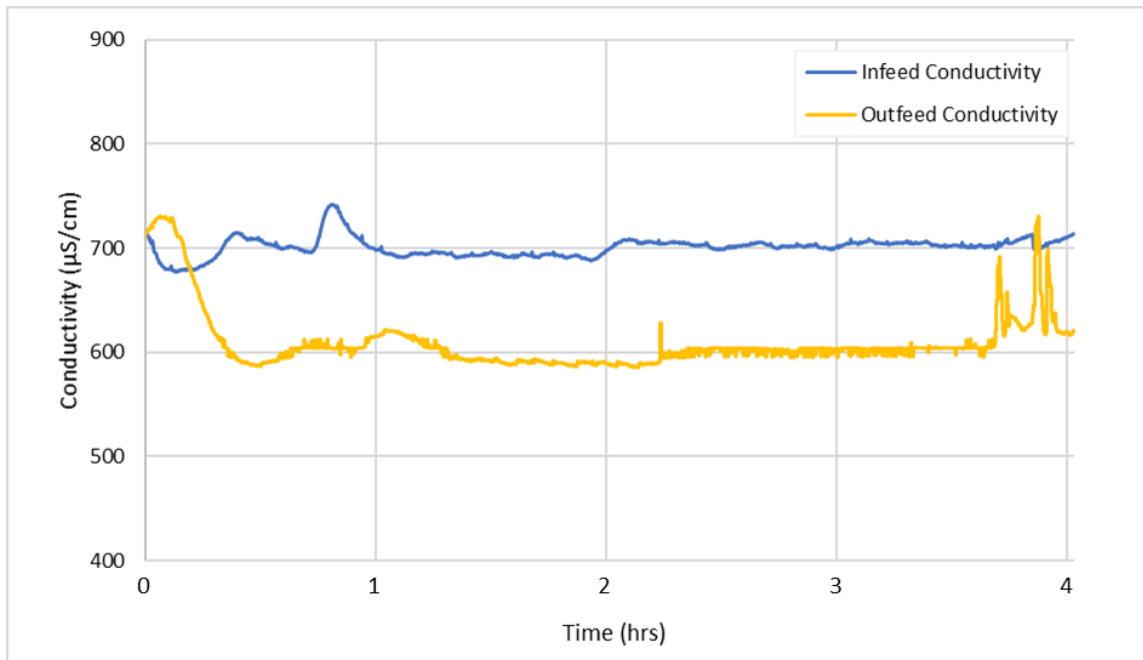


**Figure 21.** Conductivity measurements taken upstream (infeed) and downstream (outfeed) of the fluidized bed column.

The temperature profile through the fluidized bed system is plotted in Figure 22. Wine entered the system at a steady temperature, starting at  $50^\circ\text{F}$ , the temperature at which the wine is stored, and slowly increased as the tank of wine treated was no longer chilled (light green line).

Next the untreated wine passes through the heat exchanger in contact with the chilled outgoing wine; this step pre-chills the wine before it enters the chiller (light blue line). Wine exits the chiller at its lowest temperature (~30 °F, -1.1 °C) and enters the bottom of the crystallizer (grey line). After passing through the bed of crystals the wine exits the column and passes through the opposite side of the heat exchanger (brown line). After chilling the incoming wine, the treated wine approaches a temperature close to the initial storage temperature of 50 °F before exiting the system (dark blue line).

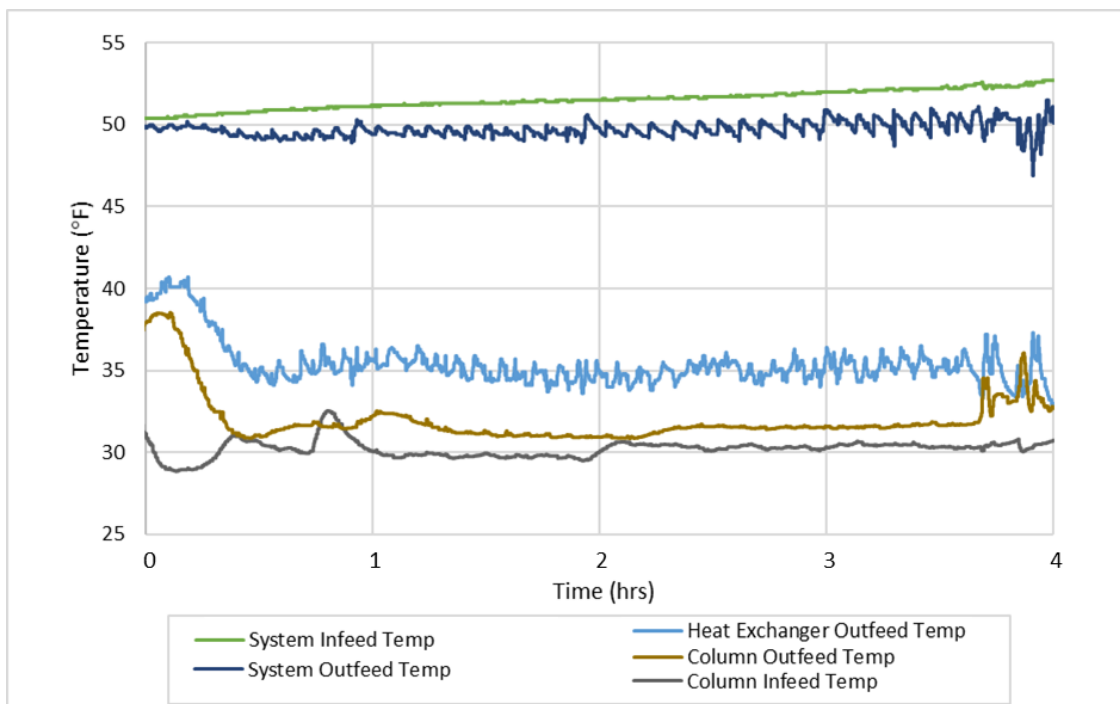


**Figure 22.** Temperature measurements taken throughout the fluidized bed system.

The majority of energy spent by the chiller was recuperated by the plate heat exchanger after the column. In this initial trial, the approximate energy recovery for the heat exchanger in this experiment was 76%, calculated by Equation 14.<sup>14</sup> Improved insulation combined with optimization of infeed flow and heat exchanger area will improve this efficiency in subsequent trials.

$$\frac{T_{feed} - T_{HX}}{T_{feed} - T_{chiller}} * 100\% \quad (14)$$

$$\frac{51\text{ }^{\circ}\text{F} - 35\text{ }^{\circ}\text{F}}{51\text{ }^{\circ}\text{F} - 30\text{ }^{\circ}\text{F}} * 100\% \approx 76\%$$

The pressure before and after the column is plotted in Figure 23. Pressure readings initially remained stable with a difference of ~3 psi accounting for the approximate 7 feet of head pressure between the transducers. Starting around the second hour the outfeed pressure began to drop steadily due to a buildup of crystals at the bottom of the mesh. Eventually the pressure difference became too large to continue, and the experiment ended after the fourth hour. A prefilter on subsequent trials removed particulates (likely naturally nucleated potassium bitartrate crystals from the feed tank) that lead to the impaction of the bottom meshed screen.

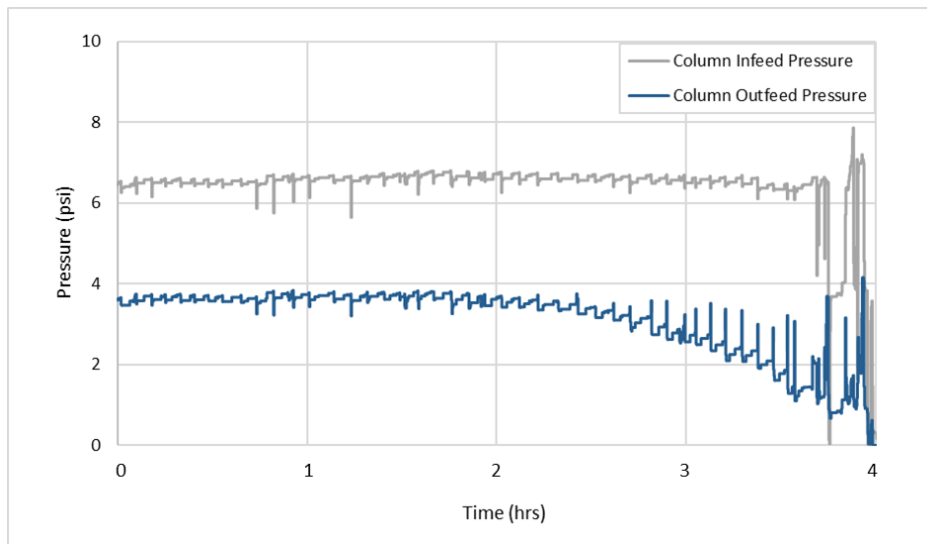


**Figure 23.** Pressure measured upstream (infeed) and downstream (outfeed) of the fluidized bed column.

The flow rate through the fluidized bed system is plotted in Figure 24. The pump was set to maintain a flow of 0.5 gallons per minute to fluidize the crystals without carrying them away in the effluent wine. Periodic spikes in the flow rate were observed and may be an error of the sensor.

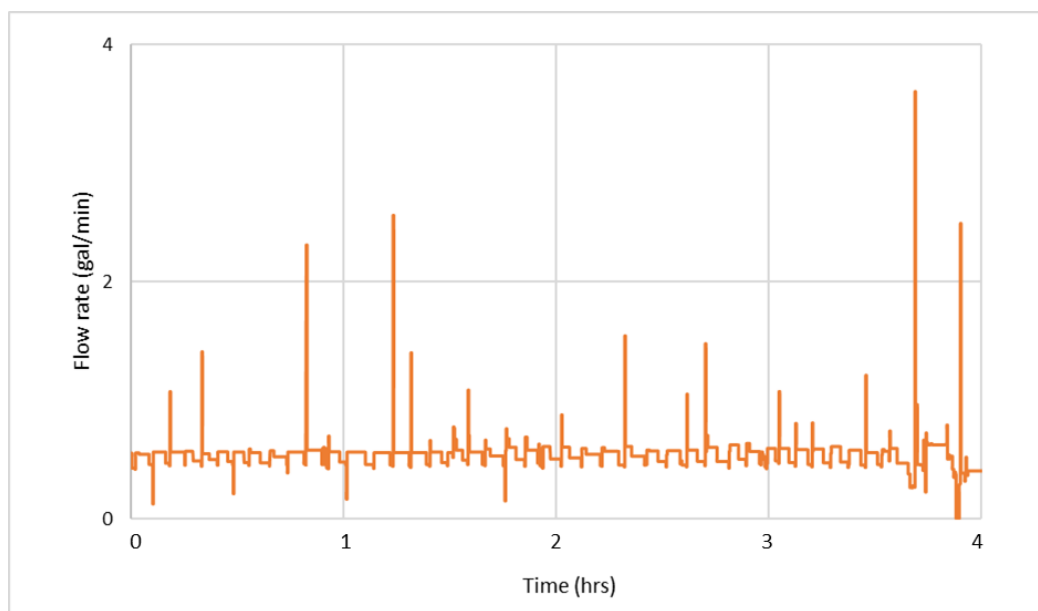
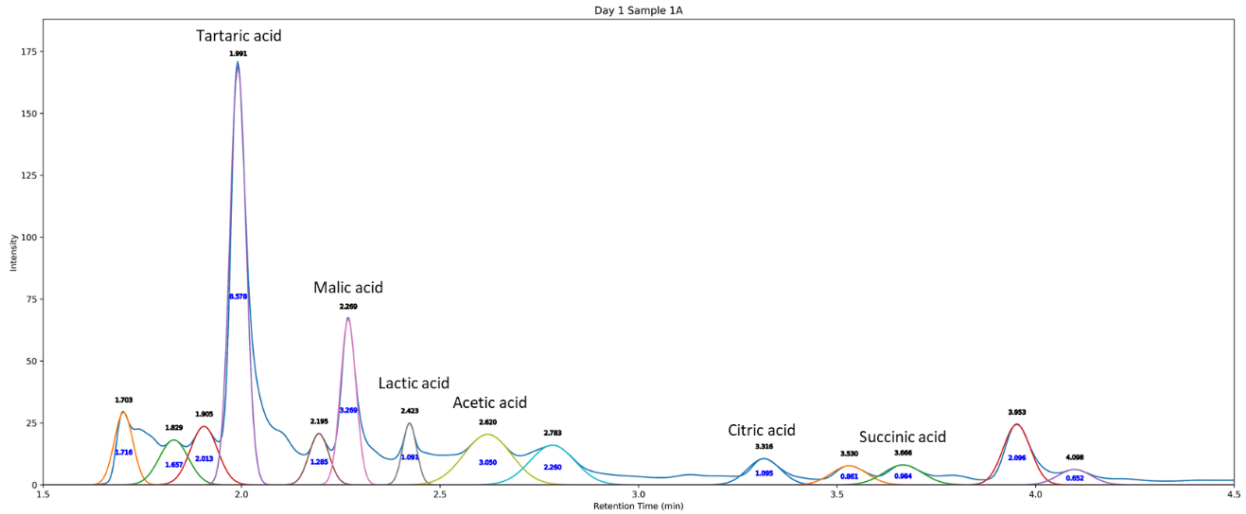


**Figure 24.** Flow rate in the fluidized bed crystallizer.

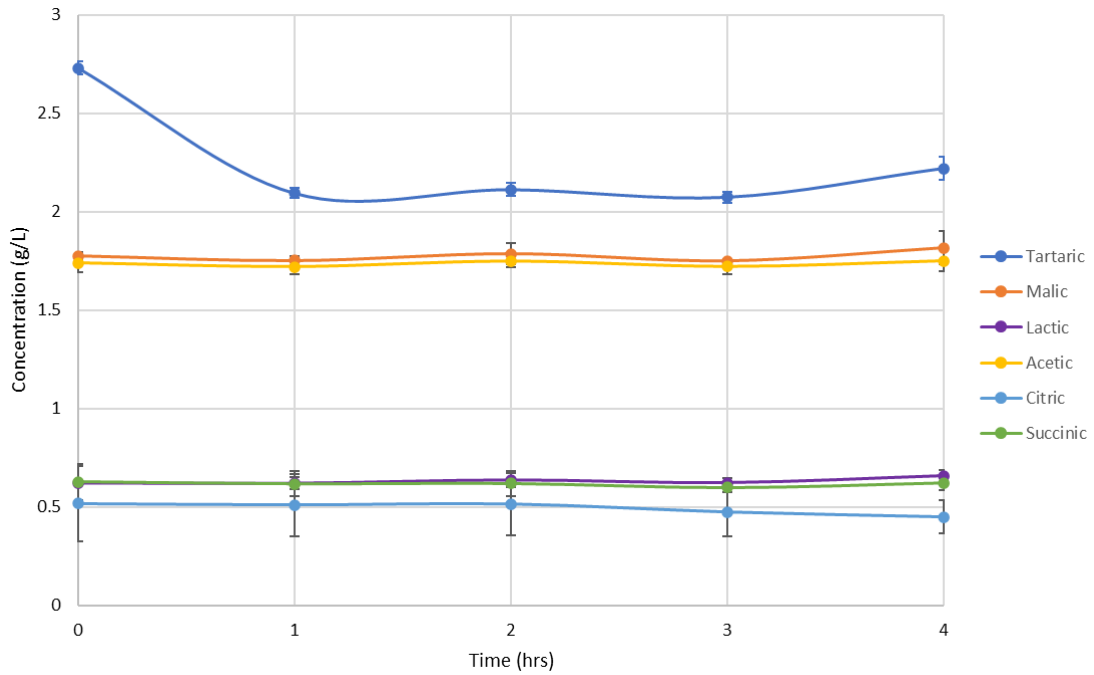
The conductivity data is useful in visualizing the removal of conductive ions from the wine, but it does not definitively reveal which ionic species are removed. To determine which molecules affected by this experiment, an organic acid analysis was performed using HPLC. An example of spectrophotometric data obtained from HPLC is shown in Figure 25. The major organic acids in wine were studied: tartaric, malic, lactic, acetic, citric, and succinic. A standard of each acid to be studied was run to determine the retention time for each acid. Samples for the untreated wine, and each hour after the experiment began, were analyzed in triplicate.

Figure 26 shows the change of the organic acid concentrations over time. Before the wine was treated, the concentration of tartaric acid was  $2.73 \pm 0.03$  g/L, the highest of all organic acids present. After an hour in the fluidized bed, the concentration of tartaric acid dropped 23% to  $2.09 \pm 0.03$  g/L, while the other acids remain stable and do not appear to significantly change. This confirms that the conductivity change observed was indeed from the removal of potassium bitartrate. By the fourth hour there was a slight increase in the concentration of tartaric acid present. Because the temperature and flowrate throughout this period is relatively constant, the decrease in

tartrate removal may be from fouling of the crystal surface from foreign material, however more tests need to be done to confirm this conclusion.



**Figure 25.** Example of HPLC spectrophotometric data



**Figure 26.** Concentration of organic acids in wine before and during treatment in the fluidized bed crystallizer. The untreated wine data are plotted at time 0 hr.

Potassium bitartrate stability over the course of the experiment was measured with a Check Stab instrument and is plotted in Figure 27. After one hour in the fluidized bed the percent change of conductivity decreased from 18% to 3.26%, demonstrating that the wine was stabilized (<5%). The fluidized bed successfully stabilized the outgoing wine for up to two hours, however, the percent change slowly increased, up to 7.74% at the fourth hour.

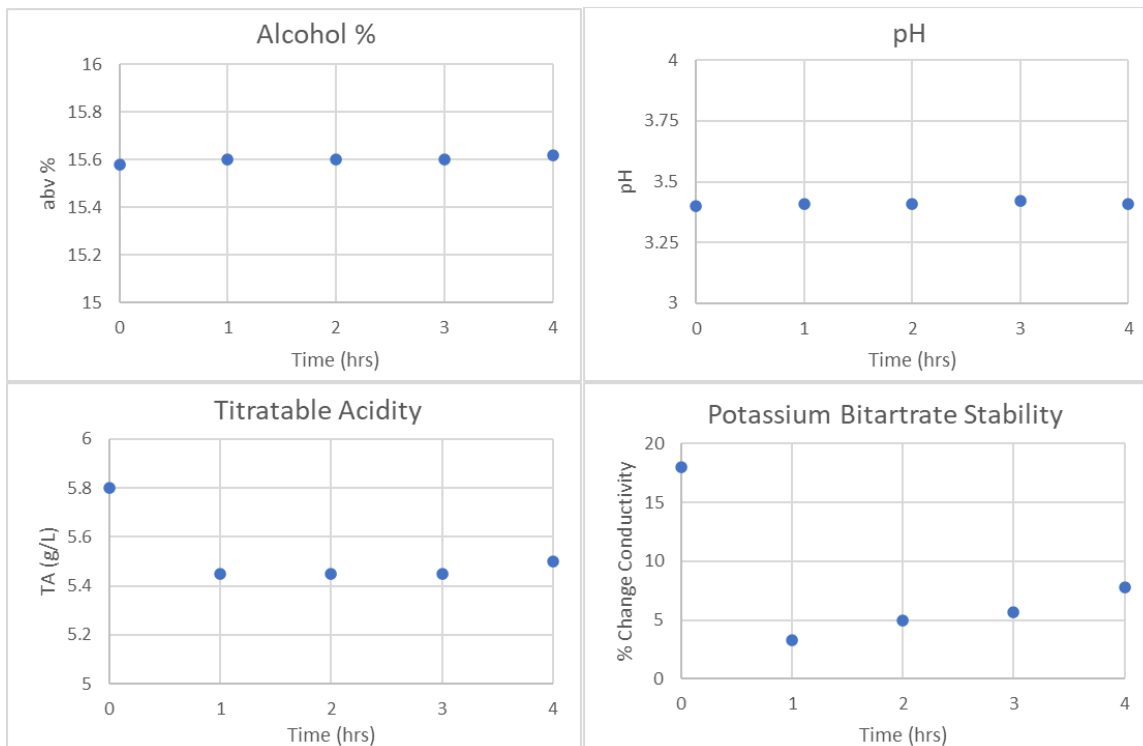


**Figure 27.** Plots of wine metrics sampled before and during treatment in the fluidized bed crystallizer.

In addition to these tests, other common quality control wine metrics are plotted in Figure 27. Alcohol content, which started at 15.58% abv, remained stable over the four hours. pH, which measures the amount of free  $H^+$  in solution also remained constant. Titratable acidity, which is a measure of total acidity in the wine, and is reflection of sour taste, showed a decrease of 6% from start to the first hour of treatment. Titratable acidity remained stably low until the last hour where a slight increase was observed.



Particle analysis before and after the experiment assessed the effects of fluidization and crystallization on the crystal particles. Histograms of maximum Feret, minimum Feret, circularity, and sphericity of the particles before and after the trial are displayed in Figure 28 and Figure 29, respectively. Tabulated values for the crystal characteristics, as well as percent change are listed in Table 3.

The average minimum Feret diameter increased 22.9%, while the average maximum Feret diameter increased 16.5%. This resulted in particles with a more circular shape. This observation was in contrast to what was expected based on particle analysis from Chapter 2. In a pure water and potassium bitartrate solution the crystal particles tended to become elongated, and sphericity decreased with size, however the opposite was true in the case of the crystals used in the treatment of this wine in a fluidized bed crystallizer. The change in crystal shape could be from surface fouling from wine colloids, which promotes growth in different directions, or from sheer friction from fluidization in the column. This outcome impacts the predictive model of fluidization by changing the particle diameter for larger crystals.

**Table 3.** Mean, standard deviation (SD), and percent change of crystal characteristics before and after 4 hours in the fluidized bed crystallizer.

Characteristic	Before		After		% Change
	Mean	SD	Mean	SD	
Maximum Feret Length	200	36	233	38	+ 16.5
Minimum Feret Length	144	21	177	27	+ 22.9
Circularity	0.77	0.084	0.822	0.062	+ 6.8
Sphericity	0.587	0.133	0.672	0.104	+ 14.5

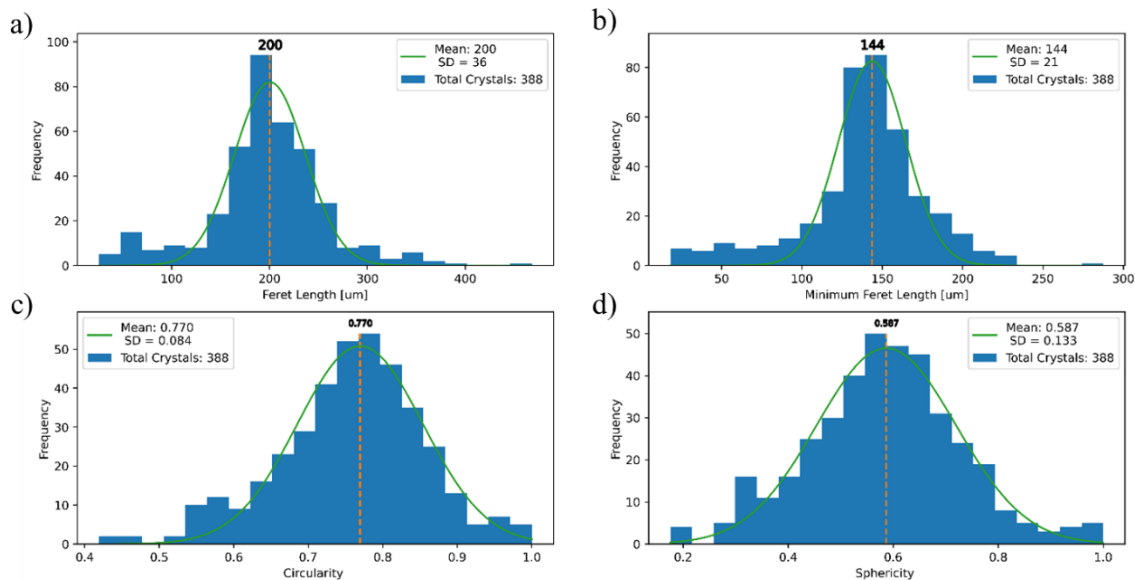


**Figure 28.** Particle analysis of crystals before use in the fluidized bed crystallizer. a) maximum Feret length, b) minimum Feret length, c) circularity, and d) sphericity.

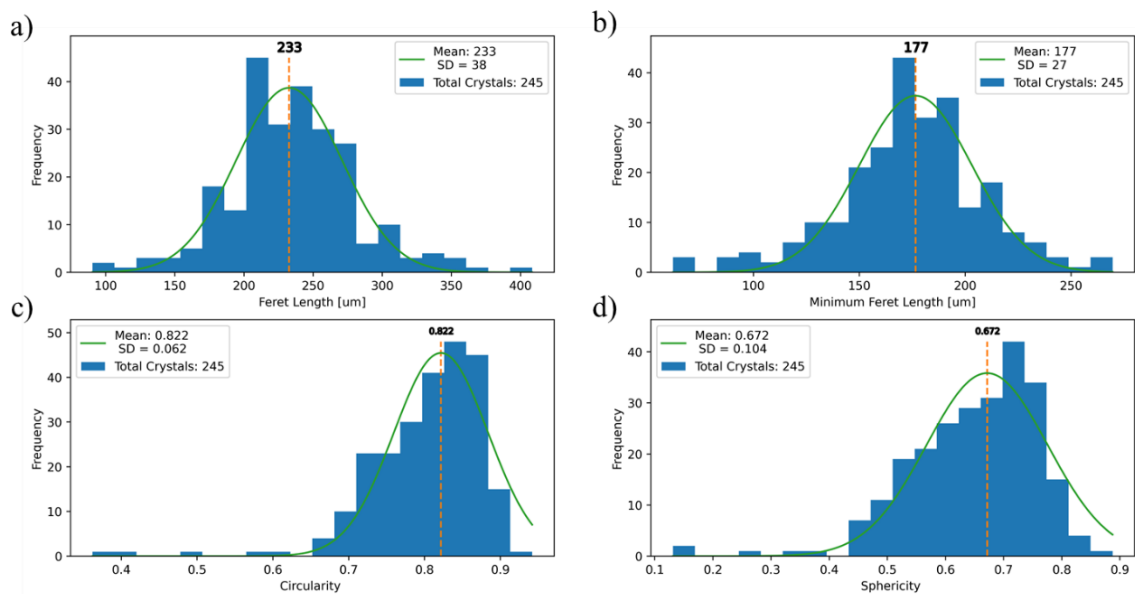


**Figure 29.** Particle analysis of crystals after use in the fluidized bed crystallizer. a) maximum Feret length, b) minimum Feret length, c) circularity, and d) sphericity.

## Conclusion

This work shows the removal of potassium bitartrate from wine with a pilot-scale fluidized bed crystallizer. The outgoing wine's electrical conductivity decreased by 14.5%, signifying a removal of ionic species. Chemical analysis by HPLC showed a decrease in tartaric acid, corresponding to the decrease in conductivity, demonstrating that the method was selective in crystallization of the desired compound. For the first two hours the effluent wine showed stability by the Check Stab test (<5% change in conductivity). A heat exchanger after the column pre-chilled the incoming wine with an approximate energy recovery of 76%, which can be improved.

Previous fluidization studies, reported in Chapter 2, examined the hydrodynamics of six various sizes of crystals, ranging from 100 – 2000  $\mu\text{m}$  in a model wine solution. Results showed that loading amount and tube diameter played an insignificant role in determining bed expansion, whereas the size of the crystals was a much more important factor. Data of bed expansion vs. superficial velocity was plotted along with the established Ergun equation for packed beds, showing the approximation is close but differs slightly because of the un-spherical morphology of the potassium bitartrate crystals. However, the results of particle analysis of crystals used for treatment of an unstable wine, show that the crystals after use may not be as un-spherical as predicted.

This research puts forth a new method of wine stabilization on a pilot-scale, improving upon the success of bench-scale potassium bitartrate removal. This early work shows fluidized bed crystallizers have the potential to be an economic and sustainable alternative to current wine industry cold stabilization practices.

## References

1. Geveke, B. J. & Runnebaum, R. C. The Future of Potassium Bitartrate Stabilization: Minimizing Energy, Wine Loss, and Treatment Time. *Catal. Discov. into Pract.* **4**, 98–106 (2020).
2. Salamone, P. & Oberholster, A. Non-subtractive approach to potassium tartrate stabilization. *Laffort/Practical Winer. Vineyard* 67–74 (2015).
3. Coulter, A. D. D. *et al.* Potassium bitartrate crystallisation in wine and its inhibition. *Aust. J. Grape Wine Res.* **21**, 627–641 (2015).
4. Berg, H. W. & Keefer, R. M. Analytical Determination of Tartrate Stability in Wine. I. Potassium Bitartrate. *Am. J. Enol. Vitic.* **9**, 180–193 (1958).
5. Sfeir, R. A. & Chow, S. Wine Cold Stabilization Energy Analysis. *Pacific Gas Electr. Co. Emerg. Technol. Progr.* (2007).
6. Nordestgaard, S., Forsyth, K., Roget, W. & O'Brien, V. Improving Winery Refrigeration Efficiency. *Aust. Wine Res. Inst.* 15 (2012).
7. Forsyth, K. AWRI Report Comparison between electro dialysis and cold treatment as a method to produce potassium tartrate stable wine Author : Karl Forsyth. 1–16 (2010).
8. Low, L. L. *et al.* Economic evaluation of alternative technologies for tartrate stabilisation of wines. *Int. J. Food Sci. Technol.* (2008). doi:10.1111/j.1365-2621.2007.01591.x
9. Karbowiak, T. *et al.* Wine Oxidation and the Role of Cork Wine Oxidation and the Role of Cork. *Crit. Rev. Food Sci. Nutr.* **8398**, (2016).
10. Sturza, R. & Covaci, E. The influence of thermal regime on stabilization process of young wines. *Sci. Study Res. Chem. Chem. Eng. Biotechnol. Food Ind.* **15**, 245–253 (2014).
11. Manns, D. C., Siricururatana, P., Padilla-Zakour, O. I. & Sacks, G. L. Decreasing pH results in a reduction of anthocyanin coprecipitation during cold stabilization of purple grape juice. *Molecules* **20**, 556–572 (2015).
12. Geankoplis, C. J. Liquid-Liquid and Fluid-Solid Separation Processes. in *Transport Processes and*

- Unit Operations* 697–753 (Prentice-Hall, Inc., 1993).
13. Bolan, R. E. Development of a Fluidized–Bed Crystallizer for Wine Treatment. (University of California – Davis, 1996).
  14. Hirzel, D. R. The Development of a Fluidized Bed for Crystallizing Potassium Bitartrate from Wine. (University of California Davis, 2008).
  15. Bosso, A. *et al.* Validation of a rapid conductimetric test for the measurement of wine tartaric stability. *Food Chem.* **212**, 821–827 (2016).
  16. Lasanta, C. & Gómez, J. Tartrate stabilization of wines. *Trends in Food Science and Technology* (2012). doi:10.1016/j.tifs.2012.06.005
  17. Bories, A. *et al.* Environmental impacts of tartaric stabilisation processes for wines using electro dialysis and cold treatment. *South African J. Enol. Vitic.* **32**, 174–182 (2011).
  18. Inamuddin & Luqman, M. Ion exchange technology II: Applications. *Ion Exch. Technol. II Appl.* **9789400740**, 1–438 (2014).
  19. Della Toffola. ‘PolarSystem’ tartaric stabilisation plant. (2008).
  20. Lankhorst, P. P. *et al.* Prevention of Tartrate Crystallization in Wine by Hydrocolloids: The Mechanism Studied by Dynamic Light Scattering. *J. Agric. Food Chem.* **65**, 8923–8929 (2017).
  21. Greeff, A. E., Robillard, B. & du Toit, W. J. Short- and long-term efficiency of carboxymethylcellulose (CMC) to prevent crystal formation in South African wine. *Food Addit. Contam. - Part A Chem. Anal. Control. Expo. Risk Assess.* **29**, 1374–1385 (2012).
  22. Sommer, S., Dickescheid, C., Harbertson, J. F., Fischer, U. & Cohen, S. D. Rationale for Haze Formation after Carboxymethyl Cellulose (CMC) Addition to Red Wine. *J. Agric. Food Chem.* **64**, 6879–6887 (2016).
  23. Younes, M. *et al.* Re-evaluation of metatartaric acid (E 353) as a food additive. *EFSA J.* **18**, (2020).
  24. Bosso, A. *et al.* Use of polyaspartate as inhibitor of tartaric precipitations in wines. *Food Chem.* **185**, 1–6 (2015).

25. Ortega-Heras, M. Mannoproteins and enology: Tartrate and protein stabilization. in *Recent Advances in Wine Stabilization and Conservation Technologies* p.95-109 (2016).
26. Guadalupe, Z., Martínez, L. & Ayestarán, B. Yeast mannoproteins in red winemaking: Effect on polysaccharide, polyphenolic, and color composition. *Am. J. Enol. Vitic.* **61**, 191–200 (2010).
27. Canuti, V., Cappelli, S., Picchi, M., Zanoni, B. & Domizio, P. Effects of high temperatures on the efficacy of potassium polyaspartate for tartaric stabilization in wines. *Am. J. Enol. Vitic.* **70**, 332–337 (2019).
28. Geankoplis, C. J. *Transport Processes and Unit Operations*. (Prentice-Hall, Inc., 1993).
29. Ergun, S. Fluid Flow Through Packed Columns. *Chem. Eng. Prog.* **48**, 89–94 (1952).
30. Merkus, H. G. *Particle Size Measurements: Fundamentals, Practice, Quality*. (Springer, 2009).
31. Dwivedi, P. N. & Upadhyay, S. N. Particle-Fluid Mass Transfer in Fixed and Fluidized Beds. *Ind. Eng. Chem. Process Des. Dev.* **16**, 157–165 (1977).
32. Kramer, O. J. I. *et al.* Accurate voidage prediction in fluidisation systems for full-scale drinking water pellet softening reactors using data driven models. *J. Water Process Eng.* **37**, 101481 (2020).
33. Karpitiski, P. H. IMPORTANCE OF THE TWO-STEP CRYSTAL GROWTH MODEL. **40**, 641–646
34. Dunsford, P. & Boulton, R. THE KINETICS OF POTASSIUM BITARTRATE CRYSTALLIZATION FROM TABLE WINES. I. EFFECT OF PARTICLE SIZE, PARTICLE SURFACE AREA AND AGITATION. (1980).
35. Waterhouse, A. L., Sacks, G. L. & Jeffery, D. W. *Understanding Wine Chemistry. Understanding Wine Chemistry* (2016). doi:10.1002/9781118730720
36. Zoecklein, B. A Review of Potassium Bitartrate Stabilization of Wines. *Virginia Polytech. Inst. State Univ. Publ.* **463**, 1–6 (1988).

## Supplemental Figures

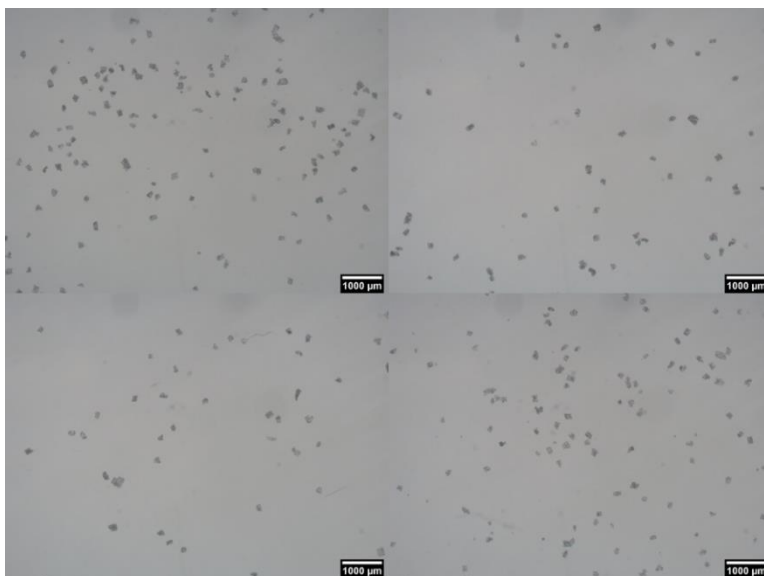


**Figure S1.** Optical microscope images of the 100  $\mu\text{m}$  nominal crystals.



**Figure S2.** Optical microscope images of the 180  $\mu\text{m}$  nominal crystals.



**Figure S3.** Optical microscope images of the 355  $\mu\text{m}$  nominal crystals.



**Figure S4.** Optical microscope images of the 710  $\mu\text{m}$  nominal crystals.



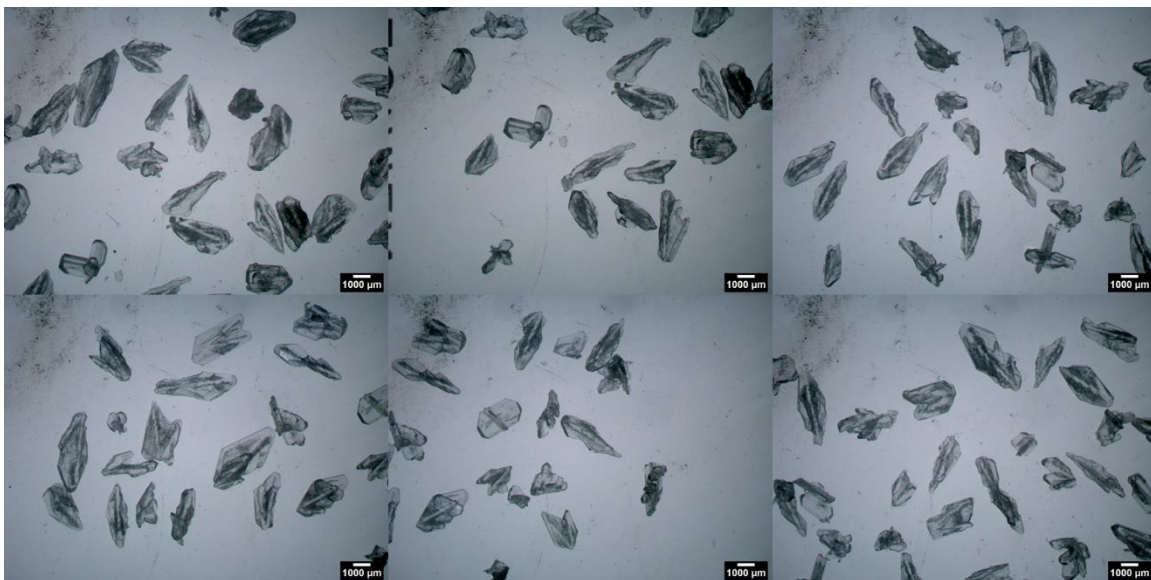


**Figure S5.** Optical microscope images of the 1000  $\mu\text{m}$  nominal crystals.

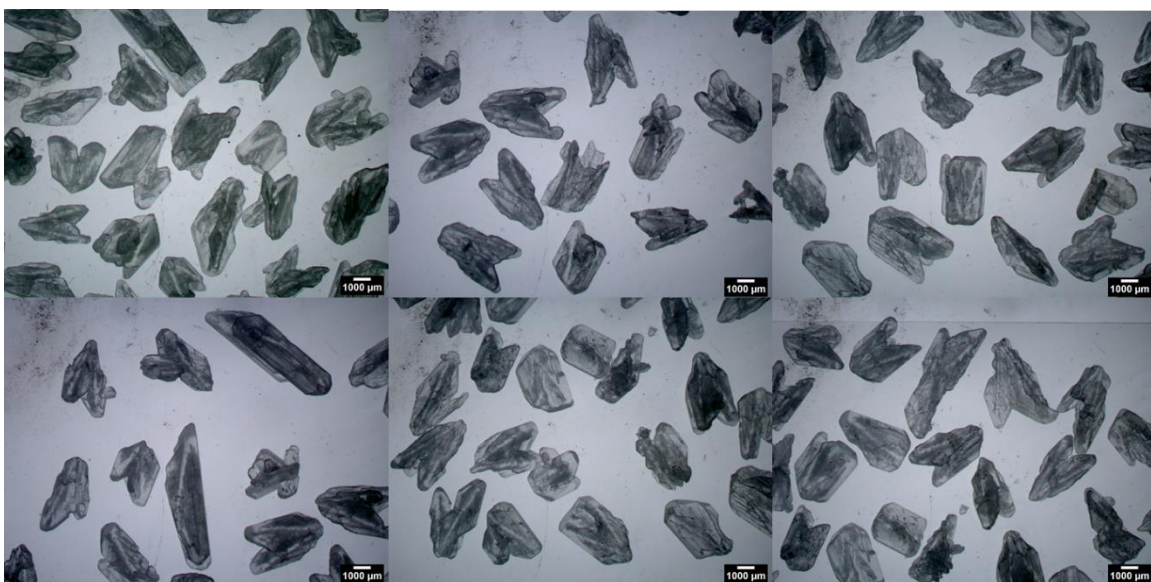


**Figure S6.** Optical microscope images of the 2000  $\mu\text{m}$  nominal crystals.



**Figure S7.** Photo of the plate heat exchanger for energy recovery.  
 a) Heat exchanger on the unit before insulation was added. b) manufacture's information plate.